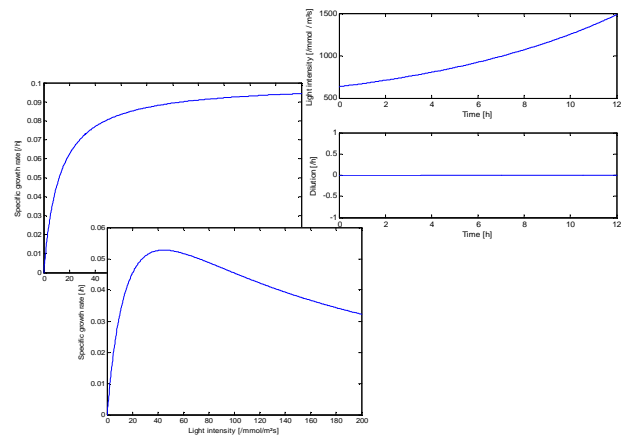
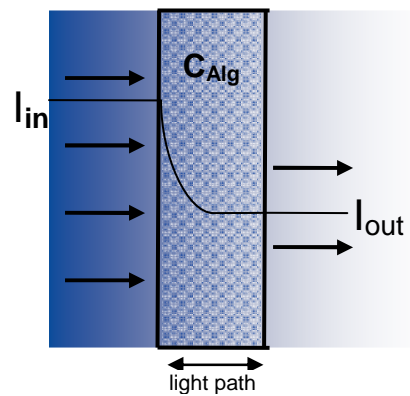


# IDENTIFICATION OF ALGAE GROWTH KINETICS

Mochamad Bagus Hermanto

May 2009





# IDENTIFICATION OF ALGAE GROWTH KINETICS

Name course : Thesis project Systems and Control  
Number : SCO-80436  
Study load : 36 ects  
Date : May 2009

Student : Mochamad Bagus Hermanto  
Registration number : 82-08-05-329-110  
Study programme : MAB (Agricultural and Bioresource Engineering)

Supervisors : dr.ir. A.J.B. Boxtel  
dr.ir. K.J. Keesman

Examiners : Prof.dr.ir. G. van Straten,  
Group : Systems and Control Group  
Address : Bornsesteeg 59  
6708 PD Wageningen  
the Netherlands  
Tel : +31 (317) 48 21 24  
Fax: +31 (317) 48 49 57



## Table of content

Title page.....	i
Table of content.....	ii
Index of figures.....	iii
Index of tables.....	iv
Acknowledgement.....	v
Summary.....	vi
1. Introduction.....	1
1.1. Problem definition.....	2
1.2. Research objectives.....	3
1.3. Research approach.....	3
1.4. Thesis outline.....	3
2. Algae photobioreactors.....	4
2.1. Photobioreactor model.....	4
2.2. Kinetic expression.....	6
2.3. Light attenuation.....	7
3. Optimal input design.....	8
3.1. Parametric sensitivity.....	8
3.2. Cost function.....	10
3.3. Dynamic optimisation.....	10
3.4. Analytical solution.....	12
3.5. Numerical methods for dynamic optimisation.....	13
3.6. Parameter estimation.....	13
4. Results.....	14
4.1. Case 1: Monod model.....	14
4.2. Case 2: Extended Monod model.....	21
4.3. Case 3: Extended Haldane model.....	24
5. Discussion.....	26
6. Conclusion and recommendations.....	27
7. List of symbols.....	28
8. References.....	29
9. Appendices.....	30
9.1. Appendix 1. Derivation of Monod and Lamber-Beer law.....	30
9.2. Appendix 2. Derivation of Haldane and Lamber-Beer law.....	31
9.3. Appendix 3. Analytical solution.....	33
9.4. Appendix 4. Tables of experimental design.....	36
9.5. Appendix 5. Program scripts.....	39

## Index of figures

Figure 1. Algae growth model .....	2
Figure 2. Algae photobioreactor .....	4
Figure 3. Specific growth rate as a function of light intensity for Monod model (a) and Haldane model (b) .....	6
Figure 4. Light attenuation in photobioreactor.....	7
Figure 5. Piecewise linear optimisation (long dash) and continuous optimisation (line).....	13
Figure 6. Precision and accuracy .....	13
Figure 7. Optimised input trajectory by using continuous optimisation with (a) $q_1:q_2 = 0:1$ which fall together with $q_1:q_2 = 1:1$ and (b) $q_1:q_2 = 1:0$ .....	15
Figure 8. Sensitivity trajectory and cost function J trajectory with (a) $q_1:q_2 = 0:1$ which fall together with $q_1:q_2 = 1:1$ and (b) $q_1:q_2 = 1:0$ .....	15
Figure 9. Optimised input trajectory by using piecewise linear with (a) $q_1:q_2 = 0:1E8$ which fall together with $q_1:q_2 = 1E8:1E8$ and (b) $q_1:q_2 = 1E8:0$ .....	15
Figure 10. Parameter estimation for weighting factor combination without noise for Case 1 .....	16
Figure 11. Sum of squares contour lines of continuous optimisation with $q_1:q_2 = 1:0$ .....	16
Figure 12. Parameter estimation for weighting factor combination with noise for Case 1 .....	16
Figure 13. Constant, stepwise, linear increasing, and optimised input of Monod model for 12 hours cultivation .....	17
Figure 14. Estimated parameters without noise application of Monod model for 12 hours cultivation .....	18
Figure 15. Estimated parameters without noise application of Monod model for 12 hours cultivation .....	18
Figure 16. Estimated parameters with 1% relative noise application of Monod model for 12 hours cultivation .....	19
Figure 17. Algae concentration as a result of optimised light intensity for Case 1 .....	19
Figure 18. Estimated parameters with 101 data points by using Monod model for 25 hours cultivation .....	19
Figure 19. Estimated parameters with 251 data points by using Monod model for 25 hours cultivation .....	20
Figure 20. Optimised input of Monod model of 25 hours cultivation .....	20
Figure 21. Optimised light intensity by using piecewise linear for Case 2 .....	21
Figure 22. Optimised input trajectory for Case 2 by using continuous optimisation .....	22
Figure 23. Algae concentration, sensitivity of parameters, cost function trajectories for Case 2 .....	22
Figure 24. Estimated parameters without noise application of extended Monod model for 12 hours cultivation .....	23
Figure 25. Estimated parameters with 1% relative noise application of extended Monod model for 12 hours cultivation .....	23
Figure 26. Input trajectories with weighting factor choices of (a) $q_1=1E8, q_2=0, q_3=0$ ; (b) $q_1=0, q_2=1E8, q_3=0$ ; (c) $q_1=0, q_2=0, q_3=1E8$ ; (d) dilution rate trajectory for all choices.....	24
Figure 27. Estimated parameters without noise application of extended Haldane model for 12 hours cultivation .....	25
Figure 28. Estimated parameters with noise application of extended Haldane model for 12 hours cultivation .....	25

## Index of tables

Table 1. Oil content of some microalgae.....	1
Table 2. Artificial light source in cultivation .....	14
Table 3. Comparison of weighting factors.....	36
Table 4. Light intensity trajectories by using Monod model with 12 hours cultivation.....	36
Table 5. Light intensity trajectories by using Monod model for 25 hours cultivation (noise free)	37
Table 6. Light intensity trajectories by using Monod model and Lambert-Beer law.....	37
Table 7. Light intensity trajectories by using Haldane model and Lambert-Beer law .....	38

## Acknowledgement

This report is the result of my major thesis work at the Systems and Control Group, Wageningen University. I am interested in the topic since it is related to algae which have big potential for renewable energy. I believe that this energy will be widely used in the future. Moreover, the model use especially Monod and Haldane kinetic model can describe the algae growth characteristic and it can be analysed through its parameter. This step is an important step to achieve in this research.

I would like to express my gratitude to all those who gave me the opportunities for doing this thesis. My sincere thanks to my supervisors Ton van Boxtel and Karel Keesman for the ideas, suggestions, and enthusiasm during my thesis work and writing this report. Without your support and guidance, I could not have completed this thesis. Many thanks to Hans Stigter for sharing his knowledge to solve the analytical solution with mathematica. I also would like to say thanks to all students who were doing their thesis in the same period with me, especially to Huda who always shared the information she had, and Rizal, Fazillah and Hassan who are motivating each other while working in the same room in Technotron building, and to all colleagues in the Systems and Control Group, who always provided me with a favourable environment for my work.

Last but not least, I would like to thank to my parent, my wife, and all my Indonesian mates for their support.

Mochamad Bagus Hermanto

May 2009

## Summary

Microalgae have high potential to be used for energy production. Growth of algae depends on inputs as light, temperature, etc. Models are needed to describe growth in algae cultivation. This thesis aims the design of experimental methods to obtain algae growth kinetics more accurate than with conventional experimental methods. The growth kinetics that concerned are Monod and Haldane. In this work, the approach to design experimental procedure is based on parametric sensitivity function.

Optimal input design method is a way to find a good estimate of parameters by designing optimal trajectories for the experimental inputs that maximize the parametric sensitivity over an experiment. Here, optimal input design is applied on three types of model which are Monod, extended Monod (Monod and Lambert-Beer law), and extended Haldane (Haldane and Lambert-Beer law). The light attenuation of light intensity inside the photobioreactor can be described by using Lambert-Beer law equation. As the inputs for the models, light intensity and dilution rate were selected.

The estimated parameters ( $\mu_{\max}$  and  $K_1$ ) were obtained for Monod and extended Monod model by using optimal input design method. Whereas, three parameters ( $\mu_{\max}$ ,  $K_1$ , and  $K_2$ ) were estimated for extended Haldane model. The correct choice of weighting factors for this optimisation was observed to reduce the confidential interval of the estimated parameters. Then, the estimated parameters were compared with the estimated parameters from intuitive input trajectories such as constant, stepwise, and linear increasing light intensity for Monod and extended Monod model. The correlation among the parameters was considered.

By giving weighting factor priority to  $K_1$  for Monod model and  $\mu_{\max}$  for Haldane model in optimisation, the best estimated parameters with low confidential interval were obtained. The optimised input trajectories in Monod and extended Monod model has the best result in parameter estimation when it is compared to intuitive input trajectories. This experimental design can minimise the confidential interval of the estimated parameters, but it did not cancel the influence of correlation. The noise at the output trajectory will significantly reduce the precision and the accuracy of the estimated parameter.

The influence of noise to the parameter estimation was observed in order to accommodate the measurement error in reality. Therefore, it is recommended to add noise filtering in order to obtain accurate estimate with low confidential interval. Another approach is also recommended to overcome the correlation problem in parameter estimation.



## 1. Introduction

The demand of fuel is increasing rapidly faster than the world population growth. The world population grew by 6.4% from 6.09 billion in 2000 to 6.48 billion in 2005 (<http://www.census.gov/ipc/www/idb/worldpop.html>), whereby, according to Energy Information Administration (EIA), the world oil consumption increased by 9.5%, from 76.712 to 84.005 million barrels per day (<http://www.eia.doe.gov/pub/international/iealf/table12.xls>). Most of the fuels used nowadays are produced from fossil fuel which is refined and burned. Significant amounts of energy are distributed among sectors like transportation, residential, commercial, and industrial. However, fossil fuel is considered as non-renewable energy where the available quantity has been decreasing.

As renewable energy source, biofuel becomes an alternative source to fulfil the daily needs. One of the emerging alternatives is biodiesel which substitutes the requirement of fossil-based for transportation and industries. Biodiesel is derived from vegetable oil which has a long carbon chain so that the viscosity becomes high. Due to the high viscosity of vegetable oil, incomplete combustion and carbon decomposition take place when it is applied directly to the engine; therefore, further processing called transesterification is needed to shorten its carbon chain structure.

Various oils have been in use in different countries as raw materials for biodiesel production. Soybean oil is commonly used in United States and rapeseed oil is used in many European countries, whereas, coconut oil and palm oils are used in Malaysia. Transesterification of edible oils has also been carried out from the oil of canola and sunflower. Other edible and non-edible oils, animal fats, algae and waste cooking oils have also been investigated by researchers for the development of biodiesel (Chisti, 2008). In fact, most of this vegetable oil is produced from plants used for food production. This development creates a competition between the use for fuel and food.

Microscopic algae often called as microalgae have fast growth and can produce lipids and have a high potential to be used for biodiesel production. Microalgae have fast growth due to its exponential growth. Oil levels of 20–50% are quite common (Table1). Oil productivity, that is the mass of oil produced per unit volume of the microalgae broth per day, depends on the algae growth rate and the oil content of the biomass. Microalgae with high oil productivities are desired for producing biodiesel (Chisti, 2007). The total oil and fat content of microalgae ranges from 1% to 70% of the dry weight and tends to be inversely proportional to the rate of growth with greater accumulations during stationary phase. The percentage of total lipid as neutral lipid, glycolipid, and phospholipid also varies widely among and within groups of microalgae (Guschina and Harwood, 2006).

**Table 1. Oil content of some microalgae**

Microalgae	Oil content (% dry wt)
<i>Botryococcus braunii</i>	25–75
<i>Chlorella</i> sp.	28–32
<i>Cryptocodinium cohnii</i>	20
<i>Cylindrotheca</i> sp.	16–37
<i>Dunaliella primolecta</i>	23
<i>Isochrysis</i> sp.	25–33
<i>Monallanthus salina</i>	> 20
<i>Nannochloris</i> sp.	20–35

Microalgae	Oil content (% dry wt)
<i>Nannochloropsis</i> sp.	31–68
<i>Neochloris oleoabundans</i>	35–54
<i>Nitzschia</i> sp.	45–47
<i>Phaeodactylum tricorutum</i>	20–30
<i>Schizochytrium</i> sp.	50–77
<i>Tetraselmis sueica</i>	15–23

Source: (Chisti, 2007)

Some factors influence the algae growth and lipid production. Photosynthetic growth requires light, carbon dioxide, water and inorganic salts. Temperature must remain generally within 20 to 30 °C (Chisti, 2007). To minimize expenses, biodiesel production must rely on freely available sunlight, despite daily and seasonal variations in light levels. Growth medium must provide the inorganic elements that constitute the algal cell. Essential elements include nitrogen (N), phosphorus (P), iron and in some cases silicon.

### 1.1. Problem definition

The interesting part of the algae cultivation is the way to control its productivity by the given inputs (light, temperature, and other operational conditions). In order to improve and to control the cultivation, models that describe the cultivation including algae growth and its kinetic expression are needed (Figure 1).

Algae growth and its kinetic expression are described by using many types of mathematical equations i.e. Michaelis-Menten or Monod equation (Grima et al., 1994; Holmberg, 1982; Rorrer and Mullikin, 1999), Haldane equation (Chisti, 2007), and Steele equation (Baquerisse et al., 1999; Benson et al., 2007).

The design of optimal inputs experiment by employing a model-based optimisation approach to estimate parameters was becoming a challenge these days. It is supposed that only light intensity and dilution are the main control inputs and other inputs, such as nutrients and the temperature remain in the optimal condition. Some experimental designs were conducted in previous studies. An experimental design which used Monod equation with constant light intensity and increased dilution rate (A-stat) as the inputs were used in optimisation of microalgae cultivation parameters (Barbosa et al., 2003). On the other hand, another experimental design which used constant light intensity and decreased dilution rate (D-stat) as the inputs was used to determine biomass yield and maintenance coefficient of phototrophic bacterium (Hoekema et al., 2006).

An alternative experimental design was proposed by using optimal parametric sensitivity control with Monod model to find the optimal input trajectory. The input is then used to estimate the parameters in the model (Stigter and Keesman, 2004). This approach for experimental design should result in the best input design which can produce accurate estimates of cultivation parameters with low confidential intervals. In this thesis we aim to test the potential for this method of the estimation of algae growth kinetic.

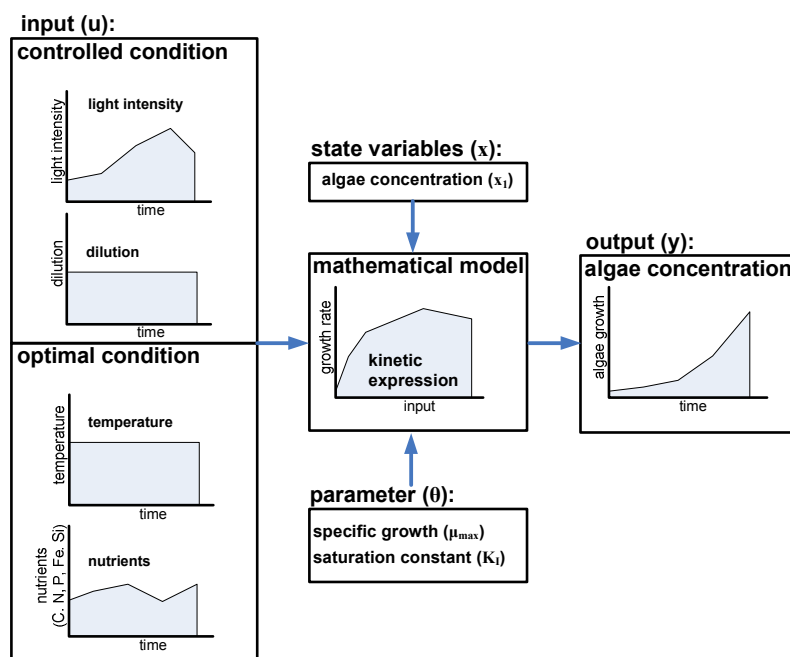


Figure 1. Algae growth model

## **1.2. Research objectives**

The research aims to evaluate the estimation of kinetic parameters in Monod and Haldane kinetic for algae growth by using optimal input design based on parametric sensitivities.

## **1.3. Research approach**

In order to accurately estimate the parameter values, the optimal input design approach was used. The optimal input design aims to find the input trajectory in such a way that the parameters are optimally estimated with low confidential intervals. Due to this problem, the optimal parametric sensitivity approach as presented by Stigter and Keesman (2004) was used as a reference in this thesis. First, Monod type kinetics with affine input is considered. An optimal input was found based on a singular control arc by applying a parametric sensitivity function and quadratic cost function using Optimal Control Theory (Bryson, 1999).

Both analytical and numerical solution approaches can be used to find the solution for optimal input. The analytical approach can be done either by hand or often symbolic manipulation with Mathematica for simple mathematical models, while, numerical solution is done either using trajectories with piecewise linear intervals or by continuous trajectories. The trajectories are obtained from the optimisation of a cost function which contains parametric sensitivity functions, where parametric sensitivity functions are added as new state variables.

The kinetic expression for growth has an effect on the trajectories for experimental design. Therefore, two growth kinetic expressions are chosen for that purpose: Monod and Haldane. For light attenuation, the law of Lambert-Beer is used.

Standard methods by using constant, stepwise, or linear increasing inputs are normally used in experimental designs. Therefore, in this work of optimal input design, these standard input strategies are compared with the optimised input in order to estimate parameters. Confidential intervals of estimated parameters are used in the evaluation of the accuracy of estimation.

## **1.4. Thesis outline**

**Chapter 1** defines the problem, research objective, and research approach.

**Chapter 2** describes mass balance, models used in this research and its kinetic expression.

**Chapter 3** explains optimal input design problem.

**Chapter 4** shows the result of some experimental designs.

**Chapter 5** discusses the results of the experiment designs.

**Chapter 6** concludes the work in this thesis and some recommendations.

## 2. Algae photobioreactors

Photobioreactors have been successfully used for producing large quantities of microalgae biomass (Chisti, 2007). In addition, photobioreactors are easy to control and permit to have single-species culture. In algae production, open pond system, flat-plate or flat panel photobioreactor, and tubular photobioreactor are used. These reactors can be operated as batch, fed-batch, and continuous bioreactor. In this thesis, a flat-plate photobioreactor system is considered.

### 2.1. Photobioreactor model

A mathematical model is a representation of a real system which is usually focused on a set of selected properties and features of the latter. Models are the essential components for modern process systems engineering methods (i.e. simulation, optimisation and control), and they are usually classified into three categories (Banga et al., 2003):

- First-principles (or white-box) models, which are derived from well known physical and chemical relationships, reflecting the underlying principles that govern the process behaviour.
- Data-driven (or black-box) models, which are of empirical nature (e.g. artificial neural networks, time series).
- Hybrid (grey-box) models: a combination of the above.

Generally, in order to develop a model, components involved in a photobioreactor system were identified and it can be described in Figure 2.

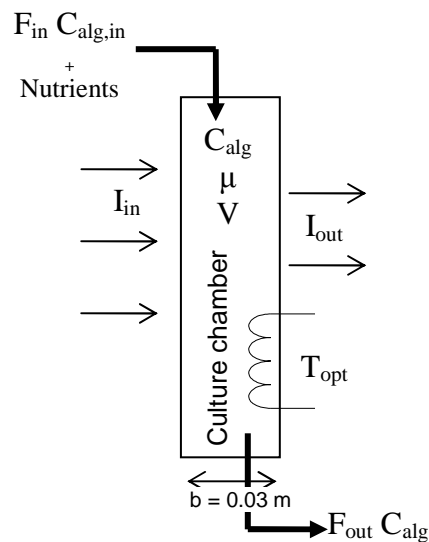


Figure 2. Algae photobioreactor

In Figure 2,  $C_{Alg}$  [ $g.l^{-1}$ ] is the algae concentration,  $F_{in\ or\ out}$  [ $l.h^{-1}$ ] the incoming or outgoing liquid flow in photobioreactor,  $\mu$  [ $h^{-1}$ ] the specific growth rate of algae,  $V$  [ $l$ ] the photobioreactor volume capacity, and  $I$  [ $\mu mol.m^{-2}s^{-1}$ ] the light intensity.

The mass balance in this system is:

$$[\text{mass accumulation}] = [\text{mass flow in}] - [\text{mass flow out}] \pm [\text{mass production or consumption}]$$

$$\frac{d[VC_{Alg}]}{dt} = F_{in} C_{Alg,in} - F_{out} C_{Alg} + \mu C_{Alg} V \quad (2-1)$$

$$V \frac{dC_{Alg}}{dt} + C_{Alg} \frac{dV}{dt} = F_{in} C_{Alg,in} - F_{out} C_{Alg} + \mu C_{Alg} V$$

The change of volume is the difference between the incoming and outgoing flow.

$$\frac{dV}{dt} = F_{in} - F_{out} \quad (2-2)$$

Substituting Equation 2-1, then:

$$V \frac{dC_{Alg}}{dt} + C_{Alg} (F_{in} - F_{out}) = F_{in} C_{Alg,in} - F_{out} C_{Alg} + \mu C_{Alg} V$$

$$V \frac{dC_{Alg}}{dt} = F_{in} C_{Alg,in} - F_{out} C_{Alg} + \mu C_{Alg} V - F_{in} C_{Alg} + F_{out} C_{Alg}$$

Because  $C_{Alg,out} = C_{Alg}$  and it assumes that no algae coming into the system ( $C_{Alg,in} = 0$ ), then:

$$\frac{dC_{Alg}}{dt} = \mu C_{Alg} - \frac{F_{in}}{V} C_{Alg} \quad (2-3)$$

In Equation 2-3, the change of algae concentration depends on two terms. The first term is called the dilution factor  $\left(D = \frac{F}{V}\right)$  and the second term is the specific growth rate of algae ( $\mu$ ) which depends on kinetic expression.

## 2.2. Kinetic expression

The kinetic expression is that part of the model which determines the specific production or consumption inside a bioreactor system. Michaelis-Menten equation is the most commonly used in biological, chemical, pharmacological, and medical processes to describe saturation phenomena. It was first applied to microbiology by Monod (Holmberg, 1982). The equation was also used as light-limited growth kinetic models with  $\mu_{\max}$  as maximum specific growth rate,  $K_I$  the saturation constant for light intensity, and  $I$  the light intensity (Barbosa et al., 2003; Grima et al., 1994).

$$\mu = \mu_{\max} \frac{I}{I + K_I} \quad (2-4)$$

For bacterial growth, a non-monotonic kinetic model, Haldane, can be used as well (Versyck et al., 1997). In the case of light-limited growth kinetic model, it becomes :

$$\mu = \mu_{\max} \frac{I}{I + K_1 + \frac{I^2}{K_2}} \quad (2-5)$$

The parameter  $K_1$  indicates how fast the optimum for the specific growth rate  $\mu_{\max}$  is reached,  $K_2$  is the inhibition parameter. The smaller  $K_2$  the larger the inhibition effect of the light intensity.

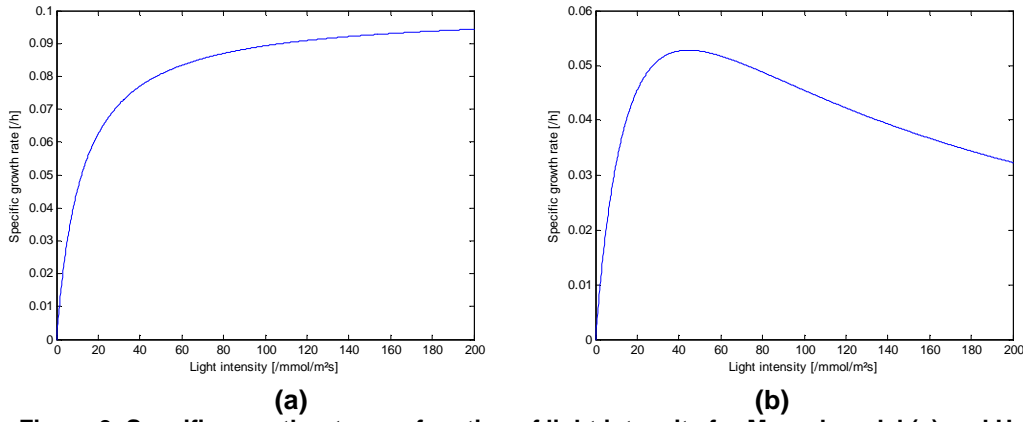


Figure 3. Specific growth rate as a function of light intensity for Monod model (a) and Haldane model (b)

Combining Equation 2-3 and Equation 2-4 leads to one state equation.

$$\frac{dC_{Alg}}{dt} = \mu_{\max} \frac{I}{I + K_I} C_{Alg} - \frac{F_{in}}{V} C_{Alg} \quad (2-6)$$

While by combining Equation 2-3 and Equation 2-5, it becomes:

$$\frac{dC_{Alg}}{dt} = \mu_{\max} \frac{I}{I + K_1 + \frac{I^2}{K_2}} C_{Alg} - \frac{F_{in}}{V} C_{Alg} \quad (2-7)$$

### 2.3. Light attenuation

Light attenuation also contributes to the algae growth limitation due to light transmission and self shading phenomena. Light intensity is decreasing along path length at photobioreactor which is presented in Figure 4. Lambert-Beer's law was used to determine the average light intensity and the light gradient inside a flat-plate photobioreactor (Barbosa et al., 2005).

$$I_{out} = I_{in} \cdot e^{-a_c \cdot C_{Alg} \cdot b} \quad (2-8)$$

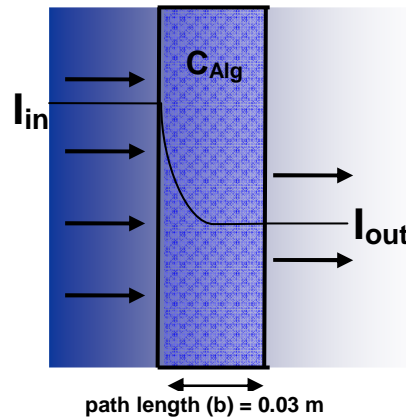


Figure 4. Light attenuation in photobioreactor

In order to find the average light intensity, integration over the path length inside the reactor yields:

$$I_{ave} = \frac{\int_0^b I_{in} \cdot e^{-a_c \cdot C_{Alg} \cdot x} dx}{\int_0^b 1 \cdot dx}$$

$$I_{ave} = I_{in} \cdot \frac{1}{b} \left( 1 - e^{-a_c \cdot C_{Alg} \cdot b} \right) \cdot \frac{1}{C_{Alg} \cdot a_c} \quad (2-9)$$

where  $b$  is photobioreactor light path and  $a_c$  is spectral-averaged absorption coefficient on a dry weight basis (Barbosa et al., 2003). The values of these constants are cited from this literature and are applied in this work:

$$b = 0.03 \text{ m}$$

$$a_c = 200 \text{ m}^2 \text{kg}^{-1}$$

### 3. Optimal input design

A good estimate of model parameters can be possibly achieved by applying optimal input design method (Stigter and Keesman, 2004). Optimal input design method is a way to find a good estimate of parameters by designing optimal trajectories for the inputs that maximize the parameter sensitivity over an experiment. In order to maximize the parameter sensitivity, the system model is extended with additional state variables related to the sensitivity function. Further, a cost function will be defined to optimize this sensitivity.

#### 3.1. Parametric sensitivity

In parametric models the output sensitivity with respect to a parameter  $\theta$  is  $\partial y/\partial\theta$ , and determines whether and how accurate a parameter can be estimated from the input/output data. In the following it is assumed, without loss of generality, that the states are directly observed so that  $y(t)=x(t)$ . If the sensitivity of  $y$  with respect to  $\theta$  is small or even zero, then the instrumentation may not be well chosen or the input sequence  $u(t)$  is not strong enough to excite the parametric sensitivities sufficiently (Stigter and Keesman, 2004).

Hence, by using the general dynamical equation:

$$\dot{x} = f(x, u, \theta, t) \quad (3-1)$$

Then, assuming  $\theta$  is time invariant, differentiation with respect to  $\theta$  and time gives:

$$\dot{x}_\theta(t) \approx \frac{\partial f}{\partial x} x_\theta(t) + \frac{\partial f}{\partial \theta} \quad (3-2)$$

i.e. the change of parametric sensitivity in time.

Applying these definitions to the algae model and by using  $x_1$  for the algae concentration  $C_{Alg}$  yields Equation 3-3 for Monod growth kinetic model or Equation 3-4 for Haldane growth kinetics model results.

$$\frac{dx_1}{dt} = \mu_{\max} \frac{I}{I + K_I} x_1 - \frac{F_{in}}{V} x_1 \quad (3-3)$$

$$\frac{dx_1}{dt} = \mu_{\max} \frac{I}{I + K_1 + \frac{I^2}{K_2}} x_1 - \frac{F_{in}}{V} x_1 \quad (3-4)$$

The numbers of the sensitivity functions depend on the number of parameters which will be estimated. In this research, three types of model are considered in three cases:

- Case 1 : Monod growth kinetic model
- Case 2 : Extended Monod growth kinetic model which is combination of Monod growth kinetic model and law of Lambert-Beer
- Case 3 : Extended Haldane growth kinetic model which is combination of Haldane growth kinetic model and law of Lambert-Beer

In Case 1, two parameters ( $\mu_{\max}$  and  $K_I$ ) will be studied. Then, for the additional state variable with respect to first parameter ( $K_I$ ):

$$x_2 = \frac{\partial x_1}{\partial K_I}$$



$$\dot{x}_2 = \frac{\partial f_1}{\partial x_1} x_2 + \frac{\partial f_1}{\partial K_I}$$

$$\frac{dx_2}{dt} = -\frac{F}{V} x_2 + \mu_{\max} \frac{I}{K_I + I} x_2 - \mu_{\max} \frac{I}{(K_I + I)^2} x_1 \quad (3-5)$$

And for the second additional state variable with respect to second parameter ( $\mu_{\max}$ ):

$$x_3 = \frac{\partial x_1}{\partial \mu_{\max}}$$

$$\dot{x}_3 = \frac{\partial f_1}{\partial x_1} x_3 + \frac{\partial f_1}{\partial \mu_{\max}}$$

$$\frac{dx_3}{dt} = -\frac{F}{V} x_3 + (x_3 \mu_{\max} + x_1) \frac{I}{K_I + I} \quad (3-6)$$

In Case 2, when light attenuation in the Monod model is considered, then the first state variable is given by substituting Equation 2-9 to Equation 3-3.

$$\frac{dx_1}{dt} = \mu_{\max} \frac{I_{in} \cdot \frac{1}{b} (1 - e^{-a_c \cdot C_{Alg} \cdot b}) \cdot \frac{1}{C_{Alg} \cdot a_c}}{\left( I_{in} \cdot \frac{1}{b} (1 - e^{-a_c \cdot C_{Alg} \cdot b}) \cdot \frac{1}{C_{Alg} \cdot a_c} \right) + K_I} x_1 - \frac{F_{in}}{V} x_1 \quad (3-7)$$

The two additional states are derived by using the symbolic toolbox and are given in Appendix 1.

In addition, Haldane growth kinetic model, three parameters ( $\mu_{\max}$ ,  $K_I$ , and  $K_2$ ) are considered in Case 3. Therefore, three additional states were added. The first state variable is given by substituting Equation 2-9 to Equation 3-4.

$$\frac{dx_1}{dt} = \mu_{\max} \frac{I_{in} \cdot \frac{1}{b} (1 - e^{-a_c \cdot C_{alg} \cdot b}) \cdot \frac{1}{C_{Alg} \cdot a_c}}{\left( I_{in} \cdot \frac{1}{b} (1 - e^{-a_c \cdot C_{alg} \cdot b}) \cdot \frac{1}{C_{Alg} \cdot a_c} \right) + K_I + \frac{\left( I_{in} \cdot \frac{1}{b} (1 - e^{-a_c \cdot C_{Alg} \cdot b}) \cdot \frac{1}{C_{Alg} \cdot a_c} \right)^2}{K_2}} x_1 - \frac{F_{in}}{V} x_1 \quad (3-8)$$

The other three additional states are derived by using the symbolic toolbox and are given in Appendix 2.

### 3.2. Cost function

The general problem optimises the cost function ( $J$ ) which is defined as:

$$J = \phi[x(t_f)] + \int_{t_0}^{t_f} L(x, u, t) dt \quad (3-9)$$

where  $\phi[x(t_f)]$  the terminal condition and  $L(x, u, p)$  the running cost; with start time  $t_0$ , final time  $t_f$ , and initial condition  $x(t_0)$  specified.

In optimal input design problem, additional state variables of parametric sensitivity need to be evaluated in time by the running cost which is part of the cost function. Weighting factors are also added in order to make priorities during optimisation. For the optimisation of the trace of the Fisher Information Matrix, we define the following quadratic cost function.

$$J = \int_{t_0}^{t_f} (q_1 s_1^2 + q_2 s_2^2 + \dots + q_n s_n^2) dt \quad (3-10)$$

where  $q_i$  is the weighting factor,  $s_i$  is the parametric sensitivity, and  $n$  is the amount of additional state variables.

Furthermore, in order to optimize the cost function itself in time, it can be added as one new additional state variable, which is known as the Mayer formulation.

$$J = x_{n+1} = \int_{t_0}^{t_f} (q_1 s_1^2 + q_2 s_2^2 + \dots + q_n s_n^2) dt \quad (3-11)$$

If the formulation is expressed into running cost of Case 1 and also at Case 2, then the equation becomes:

$$L = \frac{dx_4}{dt} = q_1 s_1^2 + q_2 s_2^2 = q_1 x_2^2 + q_2 x_3^2 \quad (3-12)$$

where  $q_1$  is the weighting factor for the parametric sensitivity  $\frac{\partial x_1}{\partial K_I}$  ( $X_2$ ) and  $q_2$  is the weighting factor for sensitivity  $\frac{\partial x_1}{\partial \mu_{\max}}$  ( $X_3$ ).

### 3.3. Dynamic optimisation

The continuous dynamic system (Equation 3-1) is described in term of the n-dimensional state vector  $x(t)$  and an m-dimensional input vector  $u(t)$  with parameter vector  $\theta$ . The optimisation problem is then to find the control vector  $u(t)$  for  $t_0 \leq t \leq t_f$  which minimizes the cost function. For this purpose Equation 3-1 is adjoined to the cost function (Equation 3-9) with a time varying Lagrange multiplier vector  $\lambda(t)$  (Bryson, 1999):

$$\bar{J} = \phi[x(t_f)] + \int_{t_0}^{t_f} \left\{ L[x(t), u(t), t] + \lambda^T(t) [f[x(t), u(t), t] - \dot{x}] \right\} dt \quad (3-13)$$

Define the scalar Hamiltonian function  $H[x(t), u(t), \lambda(t), t]$  or  $H(t)$  for compact notation:

$$H(t) = L[x(t), u(t), t] + \lambda^T(t) f[x(t), u(t), t] \quad (3-14)$$

Using Hamiltonian function (Equation 3-14) together with the integration of the term  $\lambda^T \dot{x}$  in Equation 3-13, the equation yields to:

$$\bar{J} = \phi[x(t_f)] - \lambda^T(t_f)x(t_f) + \lambda^T(t_0)x(t_0) + \int_{t_0}^{t_f} \{H[x(t), u(t), \lambda(t), t] + \lambda^T \dot{x}(t)\} dt \quad (3-15)$$

Consider an infinitesimal variation in  $u(t)$  that can be written in term of small changes  $\delta u(t)$ . Such variation will produce variations in the state histories  $\delta x(t)$  and a variation in the performance index  $\delta \bar{J}$  that could be calculated from (Bryson, 1999):

$$\delta \bar{J} = \left[ (\phi_x - \lambda^T) \delta x \right]_{t=t_f} - \left[ \lambda^T \delta x \right]_{t=t_0} + \int_{t_0}^{t_f} \left[ (H_x + \dot{\lambda}^T) \delta x + H_u \delta u \right] dt \quad (3-16)$$

To avoid having to determine the function  $\delta x(t)$  produced by  $\delta u(t)$ , the multiplier  $\lambda^T$  was chosen in such a way that the coefficients of  $\delta x(t)$  and  $\delta x(t_f)$  vanish. Bryson makes a few choices for solving this problem. The first term under the integral should be zero:

$$H_x + \dot{\lambda}^T = 0, \quad (3-17)$$

with boundary conditions

$$\lambda^T(t_f) = \phi_x(t_f). \quad (3-18)$$

Then, Equation 3-16 develops into:

$$\delta \bar{J} = \lambda^T(t_0) \delta x(t_0) + \int_{t_0}^{t_f} H_u \delta u dt \quad (3-19)$$

In order to keep  $\delta \bar{J} = 0$ ,  $H_u(t)$  must be zero and either  $\lambda^T(t_0)$  or  $\delta x(t_0)$ .  $H_u(t)$  can be interpreted as an impulse response function for  $J$ . Unit impulse in  $\delta u$  at time  $t_1$  will produce  $\delta \bar{J} = H_u(t_1)$ . Also  $\dot{\lambda}(t_0) \equiv J_x(t_0)$ , i.e.  $\lambda(t_0)$  is gradient of  $J$  with respect to  $x(t_0)$ , while holding  $u(t)$  constant and satisfying Equation 3-1. If  $x(t_0)$  is specified, then  $\delta x(t_0) = 0$ .

For a stationary solution,  $\delta \bar{J} = 0$  for arbitrary  $\delta u(t)$ ; this can only happen if:

$$H_u = 0, \quad t_0 \leq t \leq t_f. \quad (3-20)$$

Hence, to find a control vector  $u(t)$  that produces a stationary value of the cost function  $J$ , the optimisation problem must satisfy the following conditions:

State equation

$$\dot{x} = f(x, u, t) \quad (3-21)$$

Co-state equation

$$\dot{\lambda} = -H_x^T \equiv -L_x^T - f_x^T \lambda, \quad (3-22)$$

$$H_u^T \equiv L_u^T + \lambda^T f_u = 0$$

Boundary condition

$$x(t_0) = x_0, \quad (3-23)$$

$$\lambda(t_f) = \phi_x^T(t_f) \quad (3-24)$$

### 3.4. Analytical solution

In the same special cases, the solution for optimal input trajectory can be derived analytically, as is the case when light intensity is considered as the input. To solve the problem light intensity is considered to be a state variable. Therefore, two state variables are necessary: algae concentration  $x_1(t)$  and the integral of the control input  $x_2(t)$ .

$$f_1 = x_1'(t) = \frac{\mu_{\max} x_2(t)}{K_I + x_2(t)} x_1(t) \quad (3-25)$$

$$f_2 = x_2'(t) = u(t) \quad (3-26)$$

The Jacobi matrix and the parametric sensitivities are evaluated and augmented to the system:

$$\frac{\partial f}{\partial x} = \begin{bmatrix} \frac{\partial f_1}{\partial x_1} & \frac{\partial f_1}{\partial x_2} \\ \frac{\partial f_2}{\partial x_1} & \frac{\partial f_2}{\partial x_2} \end{bmatrix}$$

$$x_3 = \frac{\partial x_1}{\partial K_I}, \quad x_4 = \frac{\partial x_1}{\partial \mu_{\max}}, \quad x_5 = \frac{\partial x_2}{\partial K_I}, \quad \text{and} \quad x_6 = \frac{\partial x_2}{\partial \mu_{\max}}$$

Changing the ordering of the derivation with respect to parameters and time is allowed since the parameter is time invariant according to Equation 3-2. Consequently, we obtain:

$$\dot{x}_\theta = S = \begin{bmatrix} \frac{\partial f_1}{\partial x_1} x_3 + \frac{\partial f_1}{\partial x_2} x_5 & \frac{\partial f_1}{\partial x_1} x_4 + \frac{\partial f_1}{\partial x_2} x_6 \\ \frac{\partial f_2}{\partial x_1} x_3 + \frac{\partial f_2}{\partial x_2} x_5 & \frac{\partial f_2}{\partial x_1} x_4 + \frac{\partial f_2}{\partial x_2} x_6 \end{bmatrix} + \begin{bmatrix} \frac{\partial f_1}{\partial K_I} & \frac{\partial f_1}{\partial \mu_{\max}} \\ \frac{\partial f_2}{\partial K_I} & \frac{\partial f_2}{\partial \mu_{\max}} \end{bmatrix} \quad (3-27)$$

By considering only  $f_1$  as the function, then it becomes:

$$S = \begin{bmatrix} \frac{\partial f_1}{\partial x_1} x_3 + \frac{\partial f_1}{\partial x_2} x_5 + \frac{\partial f_1}{\partial K_I} & \frac{\partial f_1}{\partial x_1} x_4 + \frac{\partial f_1}{\partial x_2} x_6 + \frac{\partial f_1}{\partial \mu_{\max}} \end{bmatrix} \quad (3-28)$$

Thus, the equation above yields:

$$S = \left[ \frac{\mu_{\max} (x_2[t](K_I + x_2[t])x_3[t] + x_1[t](-x_2[t] + K_I x_5[t]))}{(K_I + x_2[t])^2} \quad \frac{\mu_{\max} (x_2[t](K_I + x_2[t])x_4[t] + x_1[t](K_I x_2[t] + x_2[t]^2 + K_I \mu_{\max} x_6[t]))}{(K_I + x_2[t])^2} \right]$$

The optimisation problem must satisfy the conditions from Equation 3-21 until Equation 3-24 which are given in Section 3.6. The complete solution is presented in Appendix 3 by using Mathematica. The solution is only considered for constant input trajectory. Therefore, the next sub-chapter constant input is also considered in parameter estimation.

### 3.5. Numerical methods for dynamic optimisation

Bryson developed software to find the optimum trajectories according the conditions given in Section 3-3. The problem is solved by integration. The state equation is integrated forward in time, whereas the co-state equation is integrated backward in time. This procedure continuous

until the conditions  $H_u \left( \frac{\partial H}{\partial u} \right)$  nearly zero are satisfied. The algorithm delivers for the time interval under consideration smooth continuous trajectories (see Figure 5 continuous line).

As an alternative for Bryson's method which is presented in Section 3.3, optimized trajectories can be obtained by approximation of the input trajectories by piecewise linear functions over time intervals (see Figure 5 long dash line). In this case, the optimisation concerns the values at the edges of each interval. This approach is faster than continuous optimisation since there are less interval divisions. A large value for the weighting factor is chosen due to convergence rate improvement. For this approach, *fmincon* function in Matlab is used.

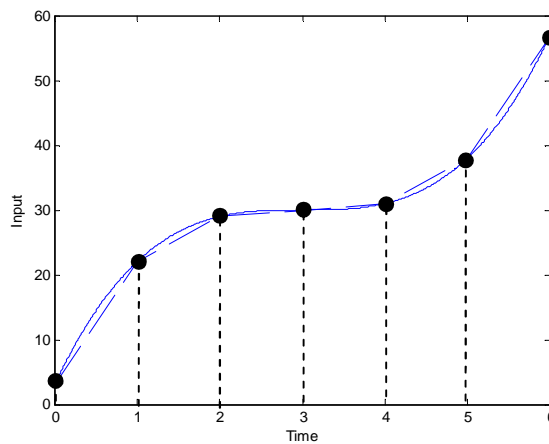


Figure 5. Piecewise linear optimisation (long dash) and continuous optimisation (line)

### 3.6. Parameter estimation

When the optimal trajectory inputs are obtained then it is used in model simulation. The obtained data with or without noise are fitted to estimate the parameters by an error norm minimisation. In this step, Matlab function *lsqnonlin* is used.

A good estimate of parameter should have high precision and high accuracy. An illustration of precision and accuracy are described in Figure 6. The precision of estimated parameters can be evaluated by confidential intervals. Therefore, confidential intervals are also calculated by using *nlparci* function in Matlab.

In this work, we only focused on having a precise estimate of the parameters by properly choosing the control input  $u(t)$ .

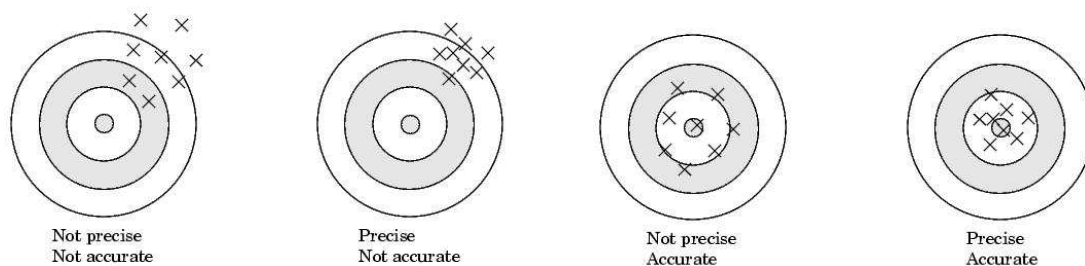


Figure 6. Precision and accuracy (Source: Matlab help files)

## 4. Results

Experimental design is made based on the model availability. In Chapter 3.1, three cases are defined based on the type of the model. Then, some constants are obtained based on previous study with *Dunaliella tertiolecta* as a model microalgae (Barbosa et al., 2003).

$$\mu_{max} = 0.09 \text{ h}^{-1}$$

$$K_I = 69.86 \text{ } \mu\text{mol.m}^{-2}.\text{s}^{-1}$$

with initial algae concentration ( $x_1(0)$ ) is  $1 \text{ g.l}^{-1}$ .

In addition, existing types of equipments which are used in experimental design have limitations on providing light. Based on Table 2, a light source range from  $0 \text{ } \mu\text{mol/m}^2\text{s}$  to  $1500 \text{ } \mu\text{mol/m}^2\text{s}$  is chosen for upper boundary in the input trajectory during the simulation.

**Table 2. Artificial light source in cultivation**

type of light source used in real practice	maximum output
red LED	2200 $\mu\text{mol/m}^2\text{s}$
red/blue LED	2800 $\mu\text{mol/m}^2\text{s}$
60 tungsten-halogen lamps	1500 $\mu\text{mol/m}^2\text{s}$

Source : Carsten Vejrazka, Kenniseenheid Agrotechniek & Voeding

### 4.1. Case 1: Monod model

A strategy to estimate two parameters ( $\mu_{max}$  and  $K_I$ ) by combining cost function's weighting factors to set a priority of optimisation is discussed. Then, a comparison of constant, stepwise, linear increasing and optimized light intensity by using Monod growth kinetic; without and with noise application are presented. Here, it is assumed that the light path is very thin, so that light extinction can be neglected.

#### 4.1.1. Choice of weighting factors

Equation 3-12 contains two weighting factors which are  $q_1$  the sensitivity of  $K_I$  and  $q_2$  the sensitivity of  $\mu_{max}$ . The optimisation is affected by  $q_1$  and  $q_2$ .

The first step, optimisation result by using  $q_1: q_2 = 0 : 1$ ;  $q_1: q_2 = 1 : 0$ ; and  $q_1: q_2 = 1 : 1$  as the weighting factors are compared.

Figure 7, for  $u_{max} = 1500 \text{ } \mu\text{mol/m}^2\text{s}$ , shows that  $q_1: q_2 = 0 : 1$  and  $q_1: q_2 = 1 : 1$  have trajectories which coincide with the upper boundary of light intensity. Whereas  $q_1: q_2 = 1 : 0$  give a unique increasing trajectory for light intensity. For all choices of the weighting factor, the optimised dilution rate is set equal to zero. This examination shows that  $q_2$  has a dominant effect in this optimisation. The reason is that the sensitivity of  $\mu_{max}$  is always much higher than the sensitivity of  $K_I$  for all the choices of weighting factors in Figure 8. Therefore, the cost function  $J$  value is dominated by  $q_2$  which also becomes high. As a consequence of the dominance is  $\mu_{max}$  will be estimated more accurately than  $K_I$ . If we want to estimate  $K_I$  accurately then it is recommended to give  $q_1$  a high value.

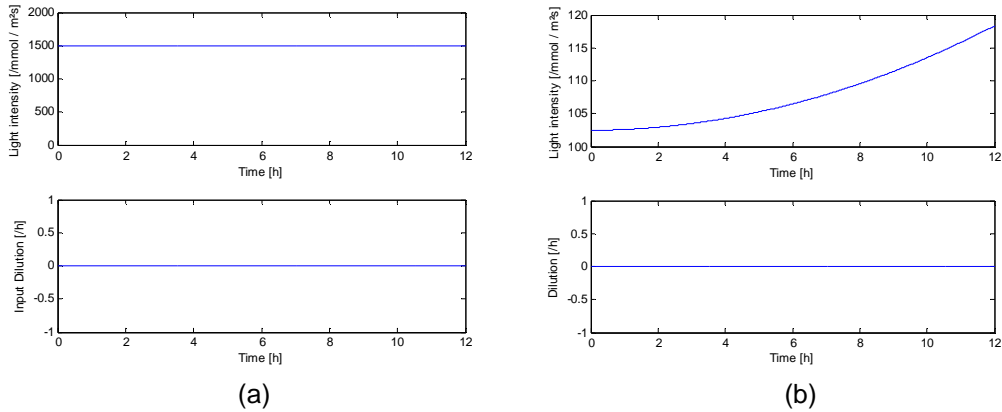


**Figure 7. Optimised input trajectory by using continuous optimisation with (a)  $q_1:q_2 = 0:1$  which fall together with  $q_1:q_2 = 1:1$  and (b)  $q_1:q_2 = 1:0$**

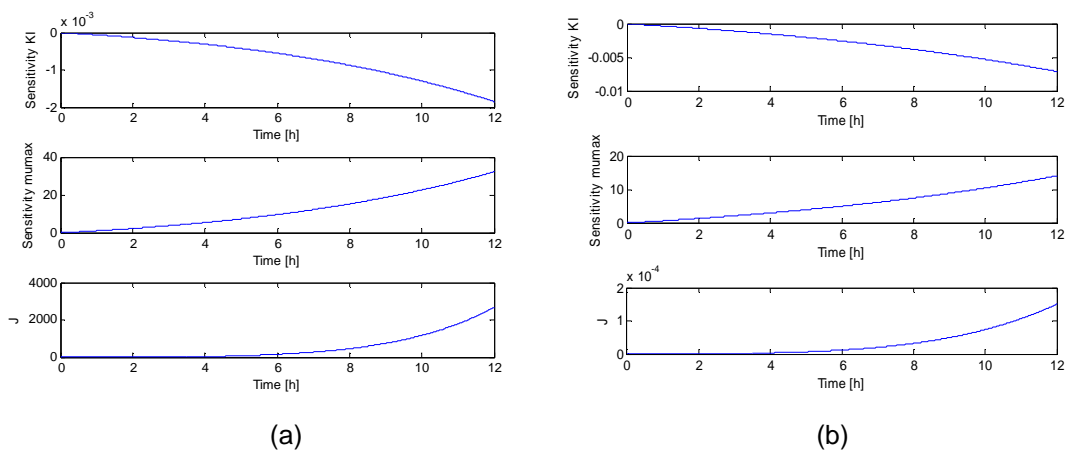


**Figure 8. Sensitivity trajectory and cost function J trajectory with (a)  $q_1:q_2 = 0:1$  which fall together with  $q_1:q_2 = 1:1$  and (b)  $q_1:q_2 = 1:0$**

Analogue with continuous optimisation, an optimised trajectory is obtained by using piecewise linear approach with weighting factor of  $q_1 : q_2 = 1E8 : 0$  with 12 intervals. A choice of large value as the weighting factor is chosen due to convergence rate improvement. This approach is conducted in order to assure the right trajectory from the continuous optimisation.

Figure 9 shows that the light intensity trajectories which are obtained by piecewise linear optimisation have similar trajectories with those which are obtained by continuous optimisation.

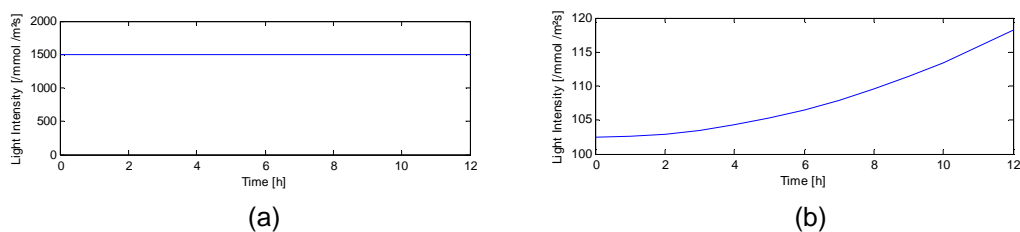


**Figure 9. Optimised input trajectory by using piecewise linear with (a)  $q_1:q_2 = 0:1E8$  which fall together with  $q_1:q_2 = 1E8:1E8$  and (b)  $q_1:q_2 = 1E8:0$**

The next step is to examine the results of the parameter estimation. The output trajectories which are used in this optimisation are obtained from optimised input trajectories with different choices of weighting factors without noise.

Obtained results are presented in Table 3 (Appendix 4) and Figure 10. By maximising only the sensitivity of  $K_1$  with the choice of  $q_1 : q_2 = 1 : 0$ , accurate and precise estimation is obtained for both  $\mu_{max}$  and  $K_1$ .

Whereas, by using the other two weighting factors choices, parameter  $\mu_{max}$  is almost accurately estimated, but it is not accurate for  $K_I$ . In addition, both estimated parameters are not precise due to a small deviation of the results.

Therefore, the weighting factor choice of  $q_1: q_2 = 1 : 0$  is recommended in order to have better estimate of both parameters.

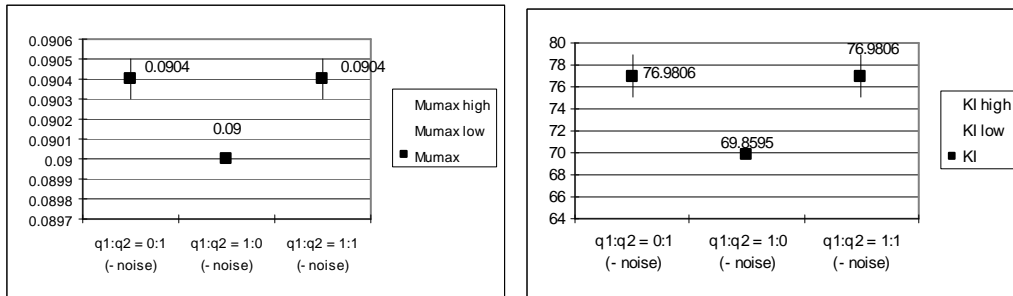


Figure 10. Parameter estimation for weighting factor combination without noise for Case 1

From Figure 11, the contour lines show that a wide range of parameter combination can be found due to the strong correlation.

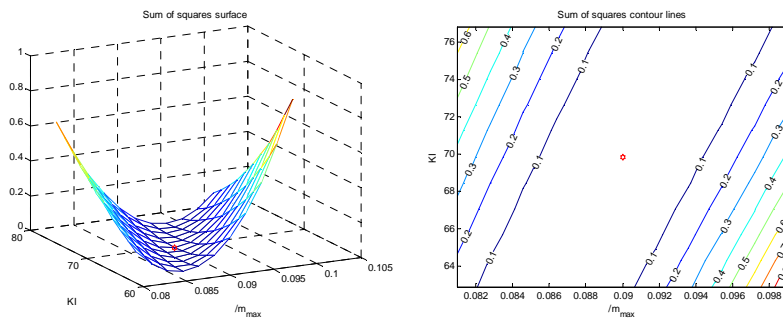


Figure 11. Sum of squares contour lines of continuous optimisation with  $q_1:q_2 = 1:0$

As the next step, parameter estimation is conducted by applying 1 % relative random noise at the output as a consequence of measurement error. Afterwards, the parameters are estimated using optimised input trajectories with different choices of weighting factors.

As a result, the parameters are not accurately estimated for all the choices of weighting factors. However, the choice of  $q_1: q_2 = 1 : 0$  gives the lowest confidential interval among the other choices. Therefore, this choice of weighting factor is recommended to estimate the parameters from noisy output trajectory. The result is presented in Figure 12 and the data is presented in Appendix 4.

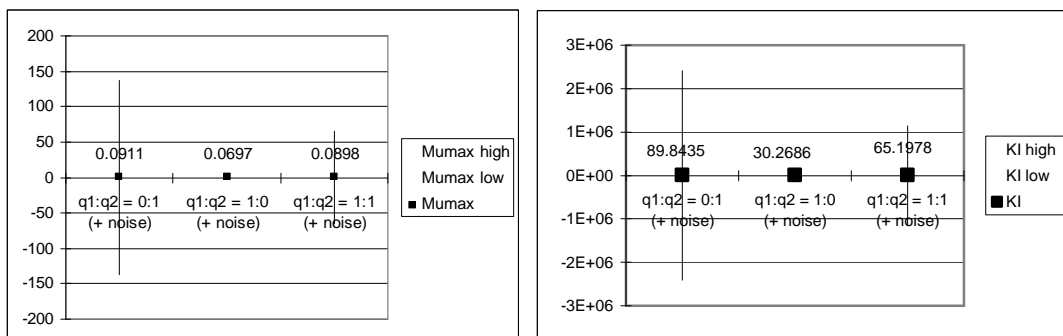


Figure 12. Parameter estimation for weighting factor combination with noise for Case 1



#### 4.1.2. Light intensity and dilution rate trajectories during optimisation

It is observed that the optimised dilution rate is zero for all weighting factor choices in Figure 7. This is a logical outcome if we regard to Equation 3-5 and Equation 3-6. It is observed that the dilution rate term ( $D = F / V$ ) has negative contribution to the maximisation of sensitivity of  $\mu_{\max}$  and sensitivity of  $K_I$ .

Whereas, it is shown that a unique trajectory is obtained as optimised light intensity depends on the weighting factors choice. This is also a logical outcome from Equation 3-5 and Equation 3-6. It is observed that light intensity ( $I$ ) has strong contribution to the maximisation of sensitivity of  $\mu_{\max}$  and sensitivity of  $K_I$ .

#### 4.1.3. Comparing optimised trajectories with alternative experimental practice

In this step, the optimised trajectories are compared with trajectories which are used in experimental practice. Three types of trajectories are considered. The applied values are derived from the optimised trajectories:

- constant light intensities are chosen which are
  - (i) at lower level of optimisation result ( $102.5 \mu\text{mol.m}^{-2}\text{s}^{-1}$ ) and
  - (ii) at upper level of optimisation result ( $118 \mu\text{mol.m}^{-2}\text{s}^{-1}$ ),
- stepwise light intensity is chosen at the lower level and the upper level of optimised trajectory,
- linear increasing light intensity is chosen from the lower level until the upper level of optimised trajectory and fourthly, the optimised trajectory by giving priority to  $K_I$ .

The effectiveness of these trajectories to estimate the kinetic parameters are compared with the optimised trajectory for  $K_I$ . For all these cases, the optimised dilution rate trajectory is zero. The trajectories are presented in Figure 13.

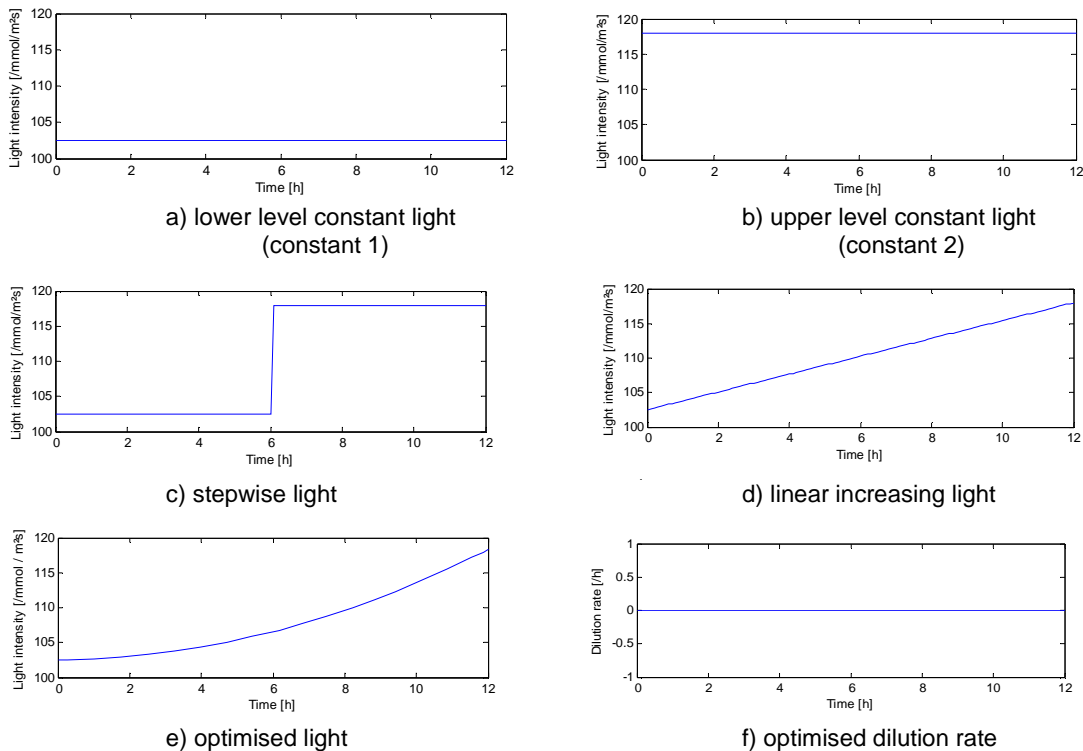


**Figure 13. Constant, stepwise, linear increasing, and optimised input of Monod model for 12 hours cultivation**

As the next step, input trajectories are used in simulation for 12 hours cultivation. The total of 101 data points of algae concentration are taken from the output trajectories without additional noise as measurement data. Afterwards, measured data are compared with the model output trajectory to extract the parameters. Obtained results are presented in Table 4 (Appendix 4).

Figure 14 shows that parameters for both parameters can be accurately estimated except for two types of constant light input trajectories.

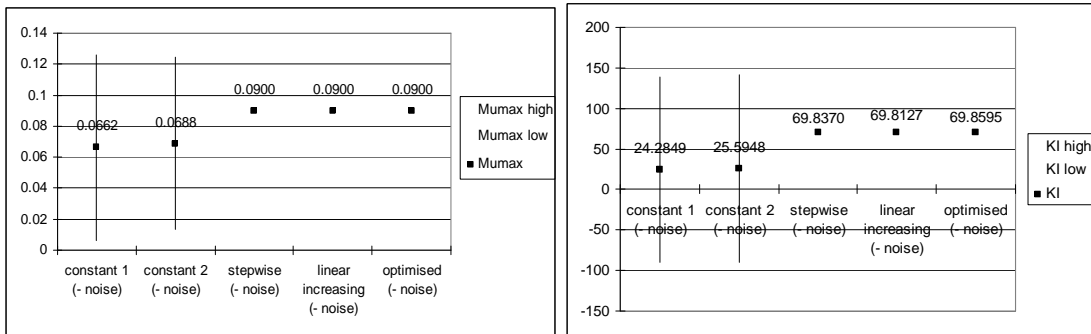


Figure 14. Estimated parameters without noise application of Monod model for 12 hours cultivation

Estimated parameters from stepwise, linear increasing, and optimised input trajectories are considered in detail in Figure 15.

It is observed that the estimate value of  $\mu_{max}$  is precisely and accurately estimated using those three input trajectories. Whereas, the estimate value of  $K_i$  is accurately estimated with the lowest confidential interval by using optimised input trajectory.

Therefore, parameter estimation by using optimised input trajectory by maximising the cost function value gives the best result under free noise condition.

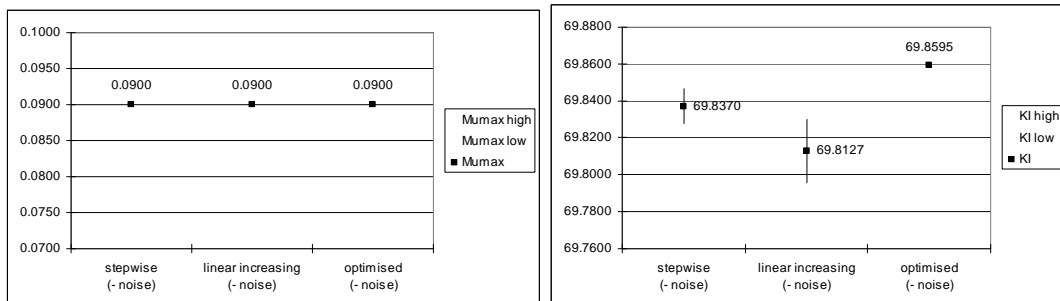


Figure 15. Estimated parameters without noise application of Monod model for 12 hours cultivation

As the last step of examination, 1 % relative noise is added as perturbation in the output for three types of light intensity trajectories. Then, total of 101 obtained data points are used as measured data and compared with the model output trajectory to extract the parameters.

The results are presented in Figure 16. Since no noise filtering in the estimation, none of parameters are accurately estimated with those three types of input trajectories. Moreover, a large deviation of the estimated parameters is obtained from the estimation. However, it can be drawn that the optimised input trajectory can reduce the noise influence and gives the smallest confidential interval among the other input trajectories.

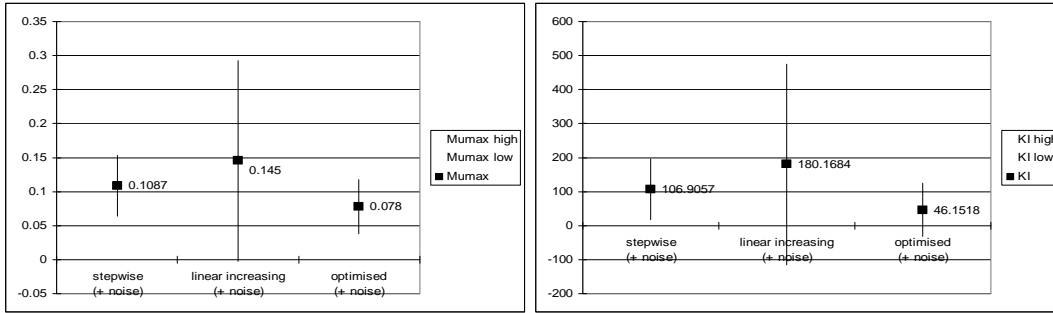


Figure 16. Estimated parameters with 1% relative noise application of Monod model for 12 hours cultivation

#### 4.1.4. The effect of additional data points and cultivation time in parameter estimation

By using the optimised input trajectory and given parameters from Barbosa et al., (2003), algae concentration increase almost twice of initial algae concentration for 12 hours cultivation and almost five times of initial algae concentration for 25 hours cultivation (Figure 17). In the following steps, comparison of additional data points and cultivation time in parameter estimation are conducted. The results are presented in Table 5 (Appendix 4).

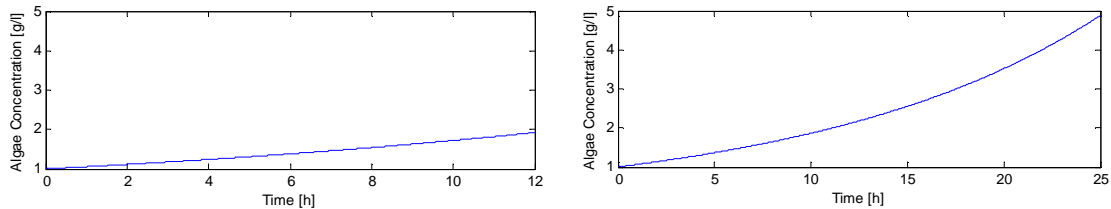


Figure 17. Algae concentration as a result of optimised light intensity for Case 1

Firstly, a comparison of parameter estimation between 12 hours cultivation and 25 hours cultivation is conducted with the same amount of data points. Three types of light intensity trajectories are compared in parameter estimation.

The estimated parameters are presented in Figure 18 for 12 hours cultivation and Figure 19 for 25 hours cultivation. As a result, the extension of cultivation time until 25 hours with 101 data points has nearly similar result with the 12 hours cultivation. The extension of cultivation time has no influence with the same data points in parameter estimation.

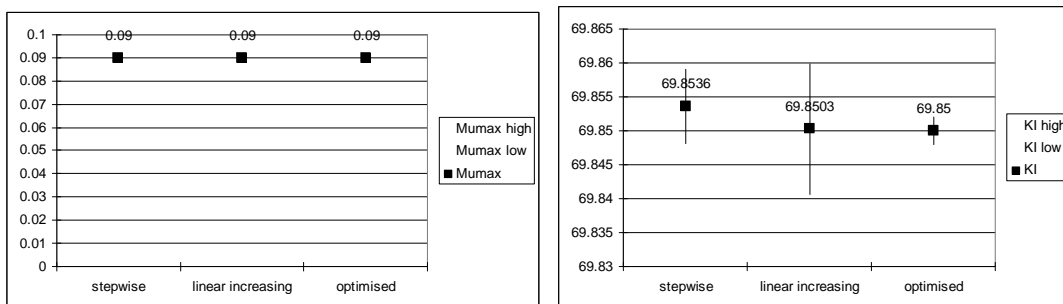
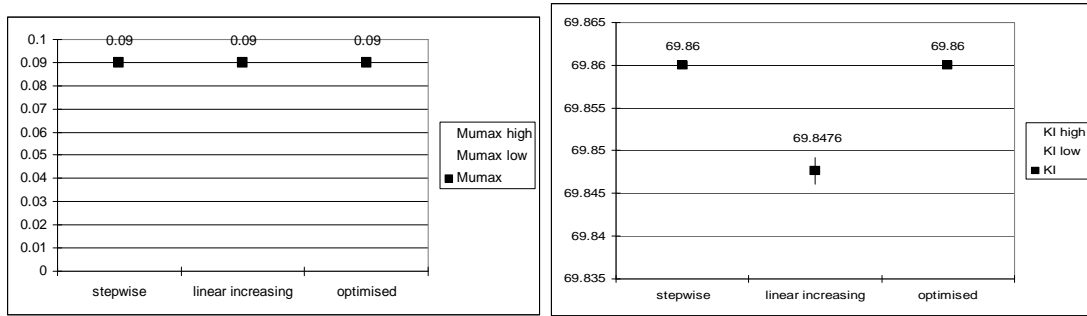


Figure 18. Estimated parameters with 101 data points by using Monod model for 25 hours cultivation

Secondly, a comparison of different amount data points with the same cultivation time is conducted. The estimated parameters with additional data points up to 251 points which are obtained from 25 hours cultivation are presented in Figure 19.

It yields that extra data points for a longer cultivation increases the accuracy and precision of estimated parameters.



**Figure 19. Estimated parameters with 251 data points by using Monod model for 25 hours cultivation**

In this case, the optimised light input trajectory in Figure 20 has the same form as in Figure 13e but the values are at higher level. Whereas, the dilution rate trajectory is zero in time.

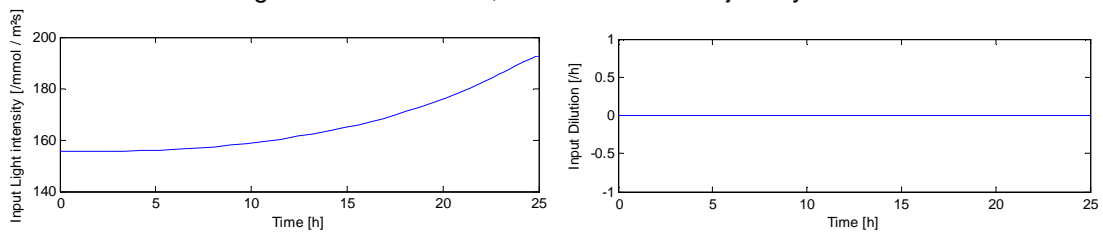


**Figure 20. Optimised input of Monod model of 25 hours cultivation**

## 4.2. Case 2: Extended Monod model

A strategy to estimate two parameters ( $\mu_{\max}$  and  $K_I$ ) for a system with light attenuation due to the algae and light transmission due to light path is considered now in combination with Monod growth kinetic. Also here a comparison of constant, stepwise, linear increasing and optimized light intensity trajectories by using extended Monod growth kinetic; without and with noise application are presented.

### 4.2.1. Optimised light intensity trajectory

A 12 linear intervals trajectory is obtained by using piecewise linear approach with weighting factor priority to  $K_I$ . It is presented in Figure 21.

In this case, the light intensity trajectory falls together with the upper boundary of light intensity after 12 hours cultivation. After that, the optimisation generates constant input in the upper level of light intensity as shown after 12 hours cultivation.

Therefore, it is concluded that a longer period than 12 hours cultivation has a trajectory that nearly a constant level at the upper boundary. And according to the result from Case 1, an accurate estimate of parameters is hardly obtained by using the constant light intensity trajectory input.

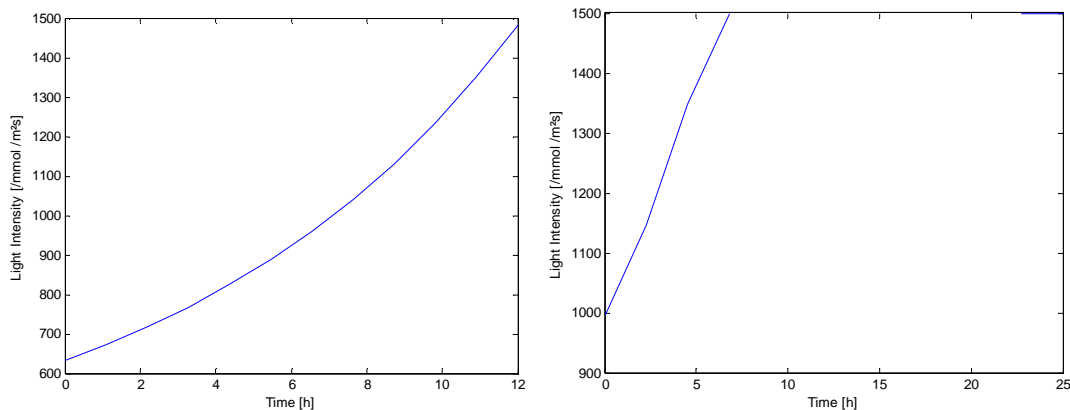


Figure 21. Optimised light intensity by using piecewise linear for Case 2

### 4.2.2. Comparing optimised trajectories with alternative experimental practice

As initial step, a continuous optimisation of 12 hours cultivation is obtained with weighting factor priority to  $K_I$ . It is presented in Figure 22a for incoming light intensity trajectory and Figure 22b for average light intensity trajectory along the path light.

It is observed that the demand of incoming optimised light intensity in Case 2 is larger than the demand of optimised light intensity in Case 1. An examination showed that the average light intensity along the light path in Case 2 is just about the same with the optimised light intensity Case 1. In addition, the optimised dilution rate of Case 2 is similar with Case 1.

Moreover, the growth rate trajectory as the function of light intensity increases quickly in the initial light intensity. Then, it increases slowly as the light intensity increases. The correlation between the growth rate and the light intensity is given in Figure 22d and e. The graphs show that the growth rate is nearly constant.

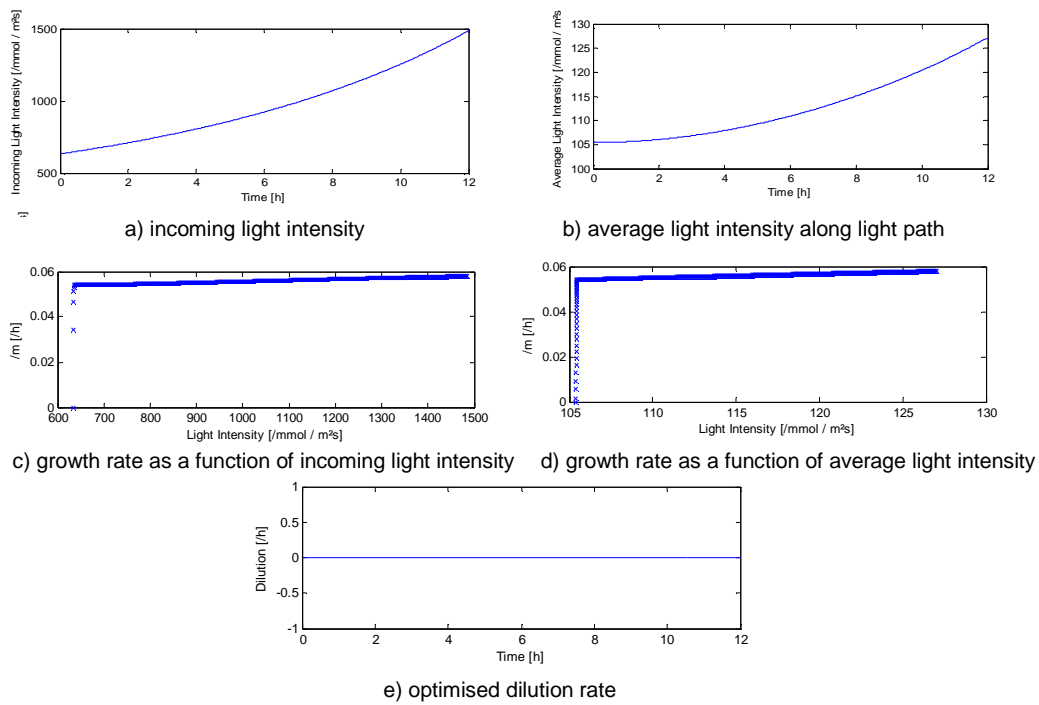


**Figure 22. Optimised input trajectory for Case 2 by using continuous optimisation**

As a result of given input during cultivation, the algae concentration in Case 2 has the same amount as in Case 1 (Figure 23). Moreover, even without giving weighting factor at  $\mu_{max}$ , it is observed in Figure 23 that the sensitivity of  $\mu_{max}$  has stronger value than the sensitivity of  $K_I$ . While the cost function  $J$  is maximised in time.

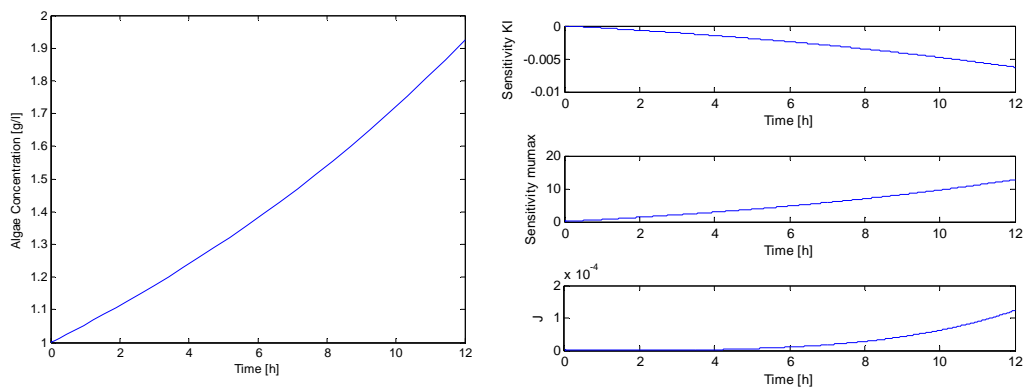


**Figure 23. Algae concentration, sensitivity of parameters, cost function trajectories for Case 2**

As the next step, parameters estimation is conducted by using continuous optimisation input trajectory. Again, the estimated parameters is compared with the estimated parameters which is obtained by using standard input trajectories which are constant, stepwise, and linear increasing light intensity. Total of 101 data points from output trajectory free noise are used in this case. The results are presented in Figure 24 and Table 6 (Appendix 4).

It is observed that all input trajectories give accurate and precise estimate of  $\mu_{max}$ . However, the estimate of  $K_I$  is accurate for constant, stepwise, and optimised light intensity trajectories. But, by using linear increasing light intensity trajectory, the estimate of  $K_I$  is not accurate with quite

high confidential interval compared to the others. Significantly, the most accurate estimate of  $K_i$  with the lowest confidential interval is obtained by using optimised trajectory.

Therefore, optimised input trajectory is recommended for accurate and precise results in extended Monod growth kinetic model.

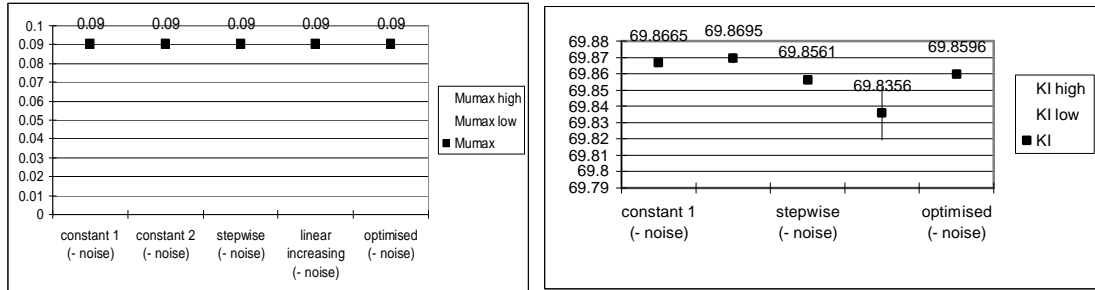


**Figure 24. Estimated parameters without noise application of extended Monod model for 12 hours cultivation**

The last step of examination, additional 1 % relative noise is added as perturbation in the output for standards light intensity trajectories and optimised light intensity trajectory. Then, total of 101 obtained data points are used as measured data and compared with the model output trajectory to extract the parameters.

The results are presented in Figure 25. Since no noise filtering in the estimation, none of parameters are accurately estimated with those input trajectories. Moreover, a large deviation of the estimated parameters is obtained from the estimation. However, it can be drawn that the noise influences the accuracy and precision of estimated parameters.

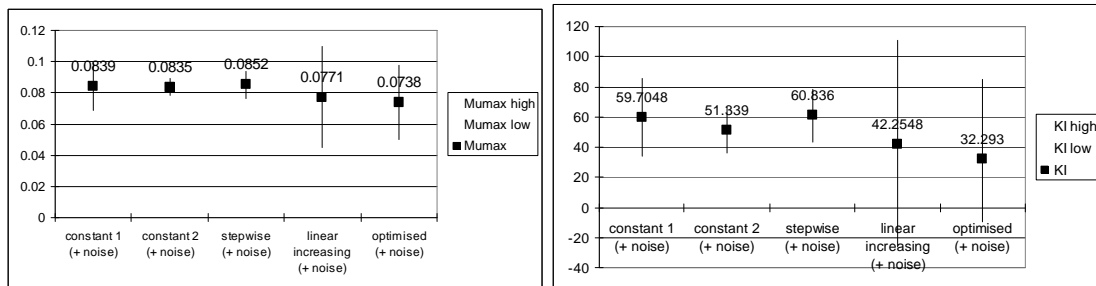


**Figure 25. Estimated parameters with 1% relative noise application of extended Monod model for 12 hours cultivation**

### 4.3. Case 3: Extended Haldane model

A strategy to estimate three parameters ( $\mu_{\max}$ ,  $K_1$ , and  $K_2$ ) in the Haldane growth kinetic is discussed. Then, the evaluation of optimized light intensity trajectories by using Haldane growth kinetic; without and with noise application are discussed.

#### 4.3.1. Choice of weighting factors

In order to estimate three parameters, three parametric sensitivity equations are needed. Therefore, three weighting factors are needed which are  $q_1$  the sensitivity of  $K_1$ ,  $q_2$  the sensitivity of  $K_2$ , and  $q_3$  the sensitivity of  $\mu_{\max}$ . The optimisation is affected by  $q_1$ ,  $q_2$ , and  $q_3$ .

The trajectory optimisation according to Bryson takes too much iteration to be successful. Therefore, the optimised input trajectories are obtained using piecewise linear approach. This optimisation is about the simple version of the continuous optimisation with limited optimisation points. The optimised light input trajectories have nearly linear increasing trajectories with different value for every choice of optimisation. It is presented in Figure 26. In all cases, the optimal dilution trajectory remains zero in time.

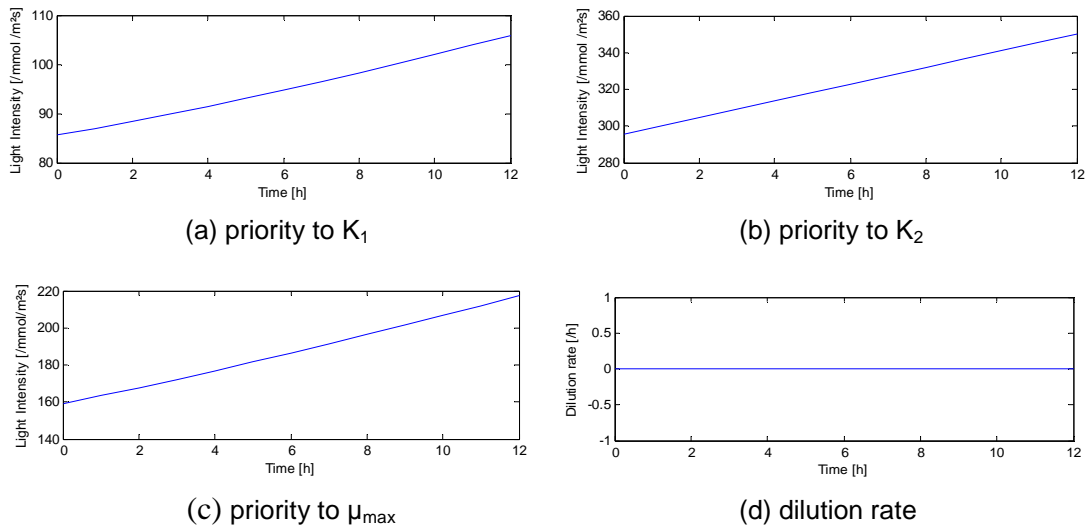


**Figure 26. Input trajectories with weighting factor choices of (a)  $q_1=1E8$ ,  $q_2=0$ ,  $q_3=0$ ; (b)  $q_1=0$ ,  $q_2=1E8$ ,  $q_3=0$ ; (c)  $q_1=0$ ,  $q_2=0$ ,  $q_3=1E8$ ; (d) dilution rate trajectory for all choices**

#### 4.3.2. Parameter estimation using optimised input

For the examination of the parameter estimation the output trajectories which are obtained from optimised input trajectories with different choices of weighting factors with and without noise application are applied.

Obtained results are presented in Table 7 (Appendix 4). The sensitivity of  $\mu_{\max}$  is more dominant among the other sensitivities. Therefore, it is shown that the choice of  $q_1=0$ ,  $q_2=0$ ,  $q_3=1E8$  has the lowest confidential interval among the other choices for both noise free (Figure 27) and with noise application (Figure 28).

Due to a strong correlation among three parameters of Haldane kinetic growth, parameter estimation of these parameters is difficult. Stepwise approach which analyse the parameter one by one can be a solution. However, it is suggested to apply it after parameter estimation with three parameters procedure in order to find every parameter with low confidential interval. Different initial guesses of parameter converge into different estimate of parameters.



In free noise case, the larger the sensitivity, the faster it converge to the expected value. The parameter  $\mu_{max}$  has the largest sensitivity value; therefore the value is close to the expected value. The results with noise seem reasonable, however, the final values ( $K_1$ ;  $K_2$ ) are close to the initial guess values. So, the identification did not improve the parameter values due to low sensitivity value of the parameters.

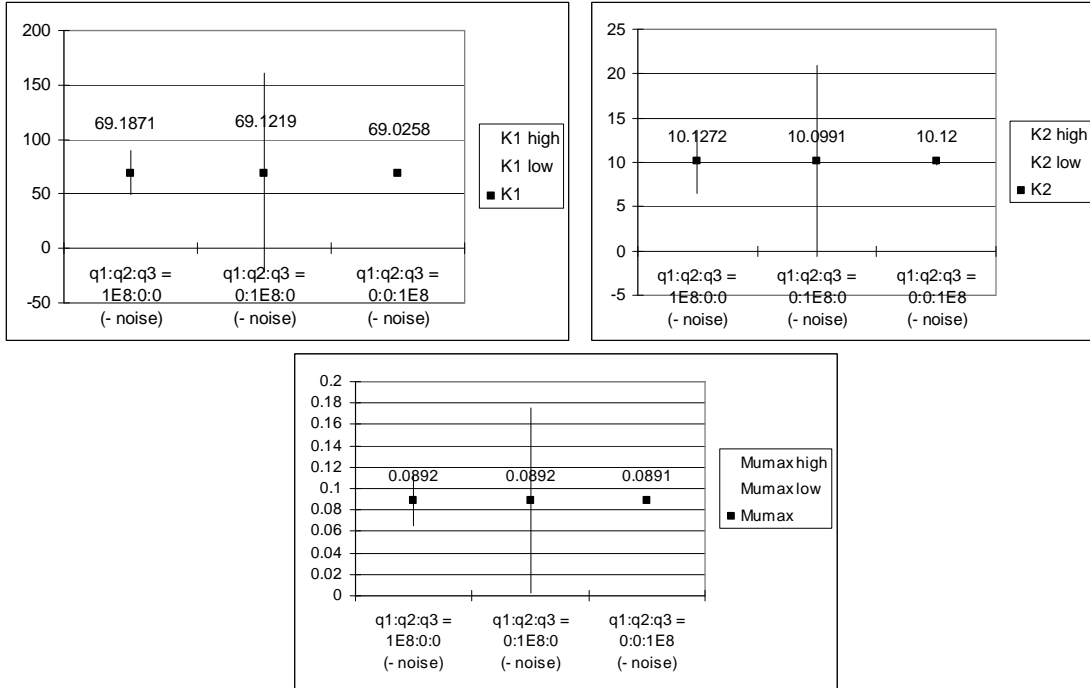


Figure 27. Estimated parameters without noise application of extended Haldane model for 12 hours cultivation

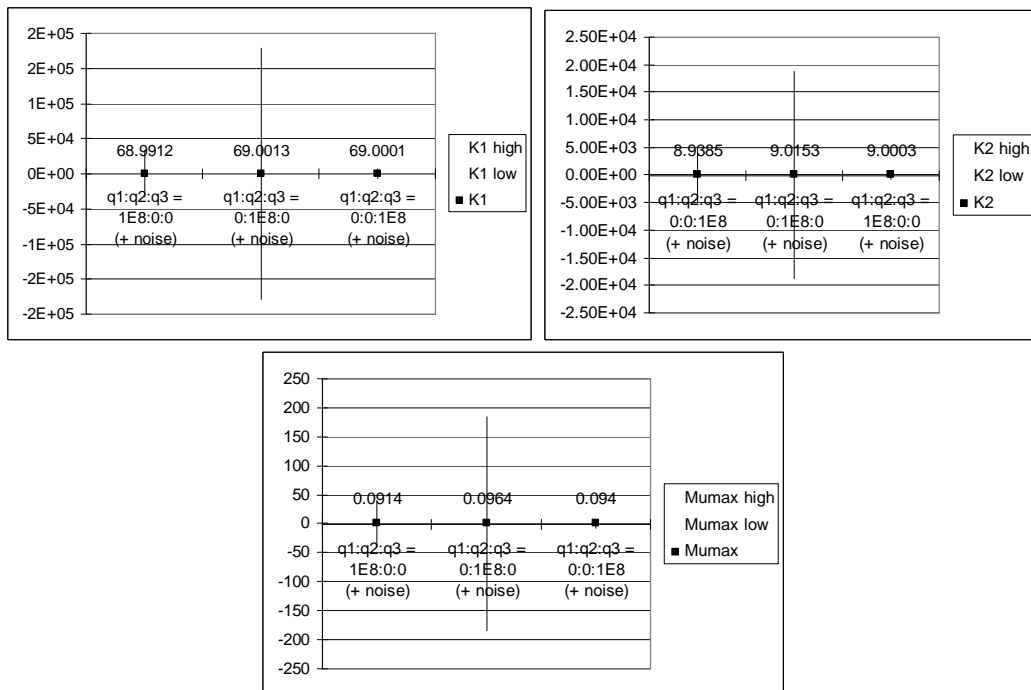


Figure 28. Estimated parameters with noise application of extended Haldane model for 12 hours cultivation

## 5. Discussion

The analytical approach was used as a starting point and yielded a constant input while the numerical optimisation methods yielded in time varying trajectories for the input. In this work, an explanation for the difference was not found. And so a further comparison of the methods is required.

For noise free experimental design, a comparison with intuitive experimental practice inputs using Monod model, the best estimate of parameters are obtained by using the optimised input trajectory. Input strategies based on stepwise input and linear increasing are better than using constant input in most of cases. By using a range of light intensity values, a range of growth rate ( $\mu$ ) can be obtained to estimate the specific growth rate ( $\mu_{\max}$ ) and saturation constant for light ( $K_l$ ). From practice, it was observed that  $\mu_{\max}$  was best estimated from high level of light intensity and  $K_l$  was best estimated from low level of light intensity.

By using extended Monod (Monod + light attenuation) model, constant inputs yielded a better estimate of parameters than linear increasing light intensity inputs at noise free experimental design which is out of the expectation (Figure 24). There is a probability that more points were laid in low level of light intensity so that the parameters especially  $K_l$  can be well estimated.

The influence of the light intensity to the light path length and algae concentration is conducted. It is observed that the light intensity demand increases along with the algae concentration and light path length. The optimum light path length is not considered for reasonable light intensity in this thesis. Therefore, a consideration of optimum light path length is important because it will influence the incoming light intensity level.

Despite trajectories for optimal sensitivity have been developed, the estimation results show a high correlation between the parameters (Figure 11). So, sensitivity optimisation improves the quality of estimation but does not cancel the correlation.

An accurate and precise estimate of parameters can be obtained by parameter estimation of Monod growth kinetic model with noise free design. However, if data is subject to noise the accuracy of the results goes down. As conducted in this research, the noise is located only at the output trajectory. The parameter estimation is conducted by using noise free input trajectories model. Therefore, noise filtering is needed in order to minimize the effect of the noise in parameter estimation.

Three types of model have been presented. For Monod model and extended Monod model, the best result of parameter estimation is obtained by giving priority to the sensitivity of  $K_l$ . While extended Haldane model, the best result of parameter estimation is obtained by giving priority to the sensitivity of  $\mu_{\max}$ .

## 6. Conclusion and recommendations

The objective of this result was to evaluate the estimation of kinetic parameters from the Monod and Haldane kinetic for algae growth by using optimal input design based on parametric sensitivity. Hereby, three models are used which are Monod model with 2 parameters, extended Monod (Monod + light attenuation) model with 2 parameters, and extended Haldane (Haldane + light attenuation) with 3 parameters.

In order to obtain the parameters, analytical and numerical approaches have been conducted. Analytical approach in this thesis is only possible for systems that are affine in the input, therefore, constant input trajectory is considered as the solution for this approach. Numerical approaches are conducted by using either continuous optimisation or piecewise linear optimisation. Both methods yield similar input trajectories.

General method which is used in this thesis is described as follows:

- a. Determine the kinetic expressions together with photobioreactor model
- b. Determine parametric sensitivity equations from the model.
- c. Obtain optimal input trajectories by analytical solution or dynamical optimisation.
- d. Estimate parameters by using optimised input trajectories.

Case 1, Monod model:

- a. Two parameters are estimated using this model which are the specific maximum growth rate  $\mu_{\max}$  and the light saturation constant  $K_I$ .
- b. The parametric sensitivity of  $\mu_{\max}$  is larger than  $K_I$ , therefore, the optimal input trajectories are depend at the weighting factors for the parameters.
- c. Giving priority of weighting factor only for  $K_I$  is the best choice to obtain optimised input trajectory for parameter estimation.
- d. Additional data from the extension of cultivation length increases the accuracy and precision of parameter estimation.

Case 2, extended Monod model:

- a. Two parameters are estimated using this model which are the specific maximum growth rate  $\mu_{\max}$  and the light saturation constant  $K_I$ .
- b. Giving priority of weighting factor only for  $K_I$  is the best choice to obtain optimised input trajectory for parameter estimation.
- c. Light intensity demand increases along with the algae concentration and light path length.

Case 3, extended Haldane model:

- a. Three parameters are estimated using this model which are the specific maximum growth rate  $\mu_{\max}$ , the light saturation constant  $K_I$ , and the inhibition constant  $K_2$ .
- b. Giving priority of weighting factor for  $\mu_{\max}$  is the best choice to obtain optimised input trajectory for parameter estimation.

For those three cases,

- a. Despite optimising the sensitivity function, the correlation between these parameters is strong, therefore, there are a wide range of parameter combination can be found.
- b. Initial guess determines the estimated parameter values, indicating the existence of local minima.
- c. Noise on measured data significantly reduces the precision and the accuracy of the estimated parameters.

In this thesis, three cases are studied in noise free and under noisy conditions. It is observed from the practice that the estimate of the parameters under noisy conditions is inaccurate and imprecise. Therefore, one of the recommendations is to add noise filtering to deal with noisy condition.

In fact, sensitivity optimisation improves the quality of estimation but does not cancel the correlation. Alternative methods are then needed to obtain more accurate parameter estimation and minimise the correlation problem.

## 7. List of symbols

notation	meaning	unit
$C_{Alg}$	algae concentration	$[g.l^{-1}]$
$C_{Alg,in}$	algae density coming into photo bioreactor	$[g.l^{-1}]$
$d$	depth of the suspension in flat-plate photobioreactor	$[m]$
$D$	dilution rate	$[h^{-1}]$
$F_{in}$	water flow coming into photo bioreactor	$[m^3.s^{-1}]$
$F_{out}$	water flow coming out from photo bioreactor	$[m^3.s^{-1}]$
$H(t)$	scalar Hamiltonian function	
$I$	light intensity	$[\mu mol.m^{-2}.s^{-1}]$
$I_{in}$	light intensity coming into photobioreactor	$[\mu mol.m^{-2}.s^{-1}]$
$I_{ave}$	average light intensity	$[\mu mol.m^{-2}.s^{-1}]$
$J$	cost function	
$K_I$	half-saturation constant for light intensity	$[\mu mol.m^{-2}.s^{-1}]$
$K_1$	half-saturation constant for light intensity	$[\mu mol.m^{-2}.s^{-1}]$
$K_2$	half-saturation constant for light intensity	$[\mu mol.m^{-2}.s^{-1}]$
$L$	running cost	
$n$	amount of additional state variables	
$q_i$	weighting factor	
$s_i$	parametric sensitivity	
$t_0$	start time	$[s]$
$t_f$	final time	$[s]$
$V$	photo bioreactor volume capacity	$[m^3]$
$x_1$	algae concentration	$[g.l^{-1}]$

Greek Letters		
notation	meaning	unit
$\alpha$	attenuation constant for glass	$[m^{-1}]$
$\phi$	terminal condition	
$\lambda$	Lagrange multiplier	
$\mu_{max}$	specific growth rate of algae at saturation	$[h^{-1}]$

## 8. References

- Banga JR, Balsa-Canto E, Moles CG, Alonso AA. 2003. Improving food processing using modern optimization methods. *Trends in Food Science & Technology* 14(4):131-144.
- Baquerisse D, Nouals S, Isambert A, dos Santos PF, Durand G. 1999. Modelling of a continuous pilot photobioreactor for microalgae production. *Journal of Biotechnology* 70(1-3):335-342.
- Barbosa MJ, Hoogakker J, Wijffels RH. 2003. Optimisation of cultivation parameters in photobioreactors for microalgae cultivation using the A-stat technique. *Biomolecular Engineering* 20(4-6):115-123.
- Barbosa MJ, Zijffers JW, Nisworo A, Vaes W, Schoonhoven Jv, Wijffels RH. 2005. Optimization of biomass, vitamins, and carotenoid yield on light energy in a flat-panel reactor using the A-stat technique. *Biotechnology and Bioengineering* 89(2):233-242.
- Benson BC, Gutierrez-Wing MT, Rusch KA. 2007. The development of a mechanistic model to investigate the impacts of the light dynamics on algal productivity in a Hydraulically Integrated Serial Turbidostat Algal Reactor (HISTAR). *Aquacultural Engineering* 36(2):198-211.
- Bryson AE. 1999. Dynamic optimization. Menlo Park, CA: Addison Wesley Longman.
- Chisti Y. 2007. Biodiesel from microalgae. *Biotechnology Advances* 25(3):294-306.
- Chisti Y. 2008. Biodiesel from microalgae beats bioethanol. *Trends in Biotechnology* 26(3):126-131.
- Grima EM, Camacho FG, Pérez JAS, Sevilla JMF, Fernández FGA, Gómez AC. 1994. A mathematical model of microalgal growth in light-limited chemostat culture. *Journal of Chemical Technology & Biotechnology* 61(2):167-173.
- Guschina IA, Harwood JL. 2006. Lipids and lipid metabolism in eukaryotic algae. *Progress in Lipid Research* 45(2):160-186.
- Hoekema S, Douma RD, Janssen M, Tramper J, Wijffels RH. 2006. Controlling light-use by *Rhodobacter capsulatus* continuous cultures in a flat-panel photobioreactor. *Biotechnology and Bioengineering* 95(4):613-626.
- Holmberg A. 1982. On the practical identifiability of microbial growth models incorporating Michaelis-Menten type nonlinearities. *Mathematical Biosciences* 62(1):23-43.
- Rorrer GL, Mullikin RK. 1999. Modeling and simulation of a tubular recycle photobioreactor for macroalgal cell suspension cultures. *Chemical Engineering Science* 54(15-16):3153-3162.
- Stigter JD, Keesman KJ. 2004. Optimal parametric sensitivity control of a fed-batch reactor. *Automatica* 40(8):1459-1464.
- Versyck KJ, Claes JE, Impe JFV. 1997. Practical Identification of Unstructured Growth Kinetic by Application of Optimal Experimental Design. *Biotechnology Progress* 13(5):524-531.

## 9. Appendices

### 9.1. Appendix 1. Derivation of Monod and Lamber-Beer law

$$dx_1dt = \frac{\mu_{max} \left( \frac{\ln^2(1/b) (1 - \exp(-ac \cdot x_1 \cdot b))}{(x_1 \cdot ac)} \right)}{\left( KI + \frac{\ln^2(1/b) (1 - \exp(-ac \cdot x_1 \cdot b))}{(x_1 \cdot ac)} \right)} \cdot x_1 - D \cdot x_1$$

$$dx_2dt =$$

$$\begin{aligned} & -(-x_2 \cdot \mu_{max} \cdot \ln \cdot \exp(-ac \cdot x_1 \cdot b) \cdot ac^2 \cdot x_1^2 \cdot b^2 \cdot KI \\ & -x_2 \cdot \mu_{max} \cdot \ln^2 \\ & +2 \cdot x_2 \cdot \mu_{max} \cdot \ln^2 \cdot \exp(-ac \cdot x_1 \cdot b) \\ & -x_2 \cdot \mu_{max} \cdot \ln^2 \cdot \exp(-2 \cdot ac \cdot x_1 \cdot b) \\ & +x_2 \cdot D \cdot KI^2 \cdot ac^2 \cdot x_1^2 \cdot b^2 \\ & +2 \cdot x_2 \cdot D \cdot KI \cdot ac \cdot x_1 \cdot b \cdot \ln \\ & -2 \cdot x_2 \cdot D \cdot KI \cdot ac \cdot x_1 \cdot b \cdot \ln \cdot \exp(-ac \cdot x_1 \cdot b) \\ & +x_2 \cdot D \cdot \ln^2 \\ & -2 \cdot x_2 \cdot D \cdot \ln^2 \cdot \exp(-ac \cdot x_1 \cdot b) \\ & +x_2 \cdot D \cdot \ln^2 \cdot \exp(-2 \cdot ac \cdot x_1 \cdot b) \\ & +\mu_{max} \cdot \ln \cdot b \cdot ac \cdot x_1^2 \\ & -\mu_{max} \cdot \ln \cdot b \cdot ac \cdot x_1^2 \cdot \exp(-ac \cdot x_1 \cdot b) \\ & / (KI \cdot ac \cdot x_1 \cdot b + \ln - \ln \cdot \exp(-ac \cdot x_1 \cdot b))^2 \end{aligned}$$

$$dx_3dt =$$

$$\begin{aligned} & -(-x_3 \cdot \mu_{max} \cdot \ln \cdot \exp(-ac \cdot x_1 \cdot b) \cdot ac^2 \cdot x_1^2 \cdot b^2 \cdot KI \\ & -x_3 \cdot \mu_{max} \cdot \ln^2 \\ & +2 \cdot x_3 \cdot \mu_{max} \cdot \ln^2 \cdot \exp(-ac \cdot x_1 \cdot b) \\ & -x_3 \cdot \mu_{max} \cdot \ln^2 \cdot \exp(-2 \cdot ac \cdot x_1 \cdot b) \\ & +x_3 \cdot D \cdot KI^2 \cdot ac^2 \cdot x_1^2 \cdot b^2 \\ & +2 \cdot x_3 \cdot D \cdot KI \cdot ac \cdot x_1 \cdot b \cdot \ln \\ & -2 \cdot x_3 \cdot D \cdot KI \cdot ac \cdot x_1 \cdot b \cdot \ln \cdot \exp(-ac \cdot x_1 \cdot b) \\ & +x_3 \cdot D \cdot \ln^2 - 2 \cdot x_3 \cdot D \cdot \ln^2 \cdot \exp(-ac \cdot x_1 \cdot b) \\ & +x_3 \cdot D \cdot \ln^2 \cdot \exp(-2 \cdot ac \cdot x_1 \cdot b) \\ & -\ln \cdot x_1^2 \cdot KI \cdot ac \cdot b - \ln^2 \cdot x_1 \\ & +2 \cdot \ln^2 \cdot x_1 \cdot \exp(-ac \cdot x_1 \cdot b) \\ & +\ln \cdot x_1^2 \cdot \exp(-ac \cdot x_1 \cdot b) \cdot KI \cdot ac \cdot b \\ & -\ln^2 \cdot x_1 \cdot \exp(-2 \cdot ac \cdot x_1 \cdot b) \\ & / (KI \cdot ac \cdot x_1 \cdot b + \ln - \ln \cdot \exp(-ac \cdot x_1 \cdot b))^2 \end{aligned}$$

## 9.2. Appendix 2. Derivation of Haldane and Lamber-Beer law

$$dx_1dt = \text{mumax} * (\text{lin} * (1/b) * (1 - \exp(-ac * x_1 * b)) * (1/(x_1 * ac))) / (K_{I1} + (\text{lin} * (1/b) * (1 - \exp(-ac * x_1 * b)) * (1/(x_1 * ac)))) + ((\text{lin} * (1/b) * (1 - \exp(-ac * x_1 * b)) * (1/(x_1 * ac)))^2 / K_{I2}) * x_1 - D * x_1$$

$$dx_2dt = - (x_2^2 * D * \text{lin}^4 + x_2 * \text{mumax} * \text{lin}^3 * \exp(-ac * x_1 * b) * b^2 * x_1^2 * ac^2 * K_{I2} - x_2 * \text{mumax} * \text{lin} * \exp(-ac * x_1 * b) * b^4 * x_1^4 * ac^4 * K_{I2}^2 * K_{I1} + x_2 * D * \text{lin}^4 * \exp(-4 * ac * x_1 * b) - 2 * x_2^2 * D * K_{I1} * b^3 * x_1^3 * ac^3 * K_{I2}^2 * \text{lin} * \exp(-ac * x_1 * b) + 6 * x_2 * \text{mumax} * \text{lin}^3 * b * ac * x_1 * K_{I2} * \exp(-ac * x_1 * b) + 2 * x_2^2 * \text{mumax} * \text{lin}^2 * b^2 * ac^2 * x_1^2 * K_{I2}^2 * \exp(-ac * x_1 * b) - 6 * x_2^2 * D * \text{lin}^3 * b * x_1 * ac * K_{I2} * \exp(-2 * ac * x_1 * b) - 4 * x_2^2 * D * \text{lin}^2 * b^2 * x_1^2 * ac^2 * K_{I2}^2 * \exp(-ac * x_1 * b) - 6 * x_2^2 * \text{mumax} * \text{lin}^3 * b * ac * x_1 * K_{I2} * \exp(-2 * ac * x_1 * b) - 4 * x_2^2 * D * K_{I1} * b^2 * x_1^2 * ac^2 * K_{I2} * \text{lin}^2 * \exp(-ac * x_1 * b) - 2 * x_2^2 * D * \text{lin}^3 * b * x_1 * ac * K_{I2} * \exp(-3 * ac * x_1 * b) + 6 * x_2^2 * D * \text{lin}^3 * b * x_1 * ac * K_{I2} * \exp(-2 * ac * x_1 * b) - x_2 * \text{mumax} * \text{lin}^2 * b^2 * ac^2 * x_1^2 * K_{I2}^2 * \exp(-2 * ac * x_1 * b) - \text{mumax} * \text{lin} * b^3 * ac^3 * x_1^4 * K_{I2}^2 * \exp(-ac * x_1 * b) - 4 * x_2^2 * D * \text{lin}^4 * \exp(-ac * x_1 * b) - 4 * x_2^2 * D * \text{lin}^4 * \exp(-3 * ac * x_1 * b) + 6 * x_2^2 * D * \text{lin}^4 * \exp(-2 * ac * x_1 * b) - 2 * x_2^2 * \text{mumax} * \text{lin}^3 * \exp(-2 * ac * x_1 * b) * b^2 * x_1^2 * ac^2 * K_{I2} + x_2 * \text{mumax} * \text{lin}^3 * \exp(-3 * ac * x_1 * b) * b^2 * x_1^2 * ac^2 * K_{I2} + 2 * x_2^2 * D * K_{I1} * b^2 * x_1^2 * ac^2 * K_{I2} * \text{lin}^2 * \exp(-2 * ac * x_1 * b) + 2 * x_2^2 * \text{mumax} * \text{lin}^3 * b * ac * x_1 * K_{I2} * \exp(-3 * ac * x_1 * b) + x_2 * D * \text{lin}^2 * b^2 * x_1^2 * ac^2 * K_{I2}^2 * \exp(-2 * ac * x_1 * b) + 2 * x_2^2 * D * \text{lin}^3 * b * x_1 * ac * K_{I2} + x_2 * D * \text{lin}^2 * b^2 * x_1^2 * ac^2 * K_{I2}^2 - x_2 * \text{mumax} * \text{lin}^2 * b^2 * ac^2 * x_1^2 * K_{I2}^2 - 2 * x_2^2 * \text{mumax} * \text{lin}^3 * b * ac * x_1 * K_{I2} + x_2 * D * K_{I1}^2 * b^4 * x_1^4 * ac^4 * K_{I2}^2 + 2 * x_2^2 * D * K_{I1} * b^3 * x_1^3 * ac^3 * K_{I2}^2 * \text{lin} + 2 * x_2^2 * D * K_{I1} * b^2 * x_1^2 * ac^2 * K_{I2} * \text{lin}^2 + \text{mumax} * \text{lin} * b^3 * ac^3 * x_1^4 * K_{I2}^2) / (K_{I1} * b^2 * x_1^2 * ac^2 * K_{I2} + \text{lin} * b * x_1 * ac * K_{I2} - \text{lin} * b * x_1 * ac * K_{I2} * \exp(-ac * x_1 * b) + \text{lin}^2 - 2 * \text{lin}^2 * \exp(-ac * x_1 * b) + \text{lin}^2 * \exp(-2 * ac * x_1 * b)) ^2$$

$$dx_3dt = - (x_3^2 * D * \text{lin}^4 * \exp(-4 * ac * x_1 * b) - 4 * x_3^2 * D * \text{lin}^4 * \exp(-3 * ac * x_1 * b) + 6 * x_3^2 * D * \text{lin}^4 * \exp(-2 * ac * x_1 * b) + 6 * x_3^2 * D * \text{lin}^3 * b * x_1 * ac * K_{I2} * \exp(-2 * ac * x_1 * b) - 2 * x_3^2 * D * \text{lin}^2 * b^2 * x_1^2 * ac^2 * K_{I2}^2 * \exp(-ac * x_1 * b) - 6 * x_3^2 * D * \text{lin}^3 * b * x_1 * ac * K_{I2} * \exp(-ac * x_1 * b) - 3 * \text{mumax} * \text{lin}^3 * b * ac * x_1^2 * \exp(-2 * ac * x_1 * b) - 4 * x_3^2 * D * \text{lin}^4 * \exp(-ac * x_1 * b) + x_3^2 * D * \text{lin}^2 * b^2 * x_1^2 * ac^2 * K_{I2}^2 * \exp(-2 * ac * x_1 * b) - 6 * x_3^2 * \text{mumax} * \text{lin}^3 * b * ac * x_1 * K_{I2} * \exp(-2 * ac * x_1 * b) + 3 * \text{mumax} * \text{lin}^3 * b * ac * x_1^2 * \exp(-ac * x_1 * b) - x_3 * \text{mumax} * \text{lin} * \exp(-ac * x_1 * b) * b^4 * x_1^4 * ac^4 * K_{I2}^2 * K_{I1} + x_3 * \text{mumax} * \text{lin}^3 * \exp(-ac * x_1 * b) * b^2 * x_1^2 * ac^2 * K_{I2} + 2 * x_3^2 * \text{mumax} * \text{lin}^2 * b^2 * ac^2 * x_1^2 * K_{I2}^2 * \exp(-ac * x_1 * b) + 6 * x_3^2 * \text{mumax} * \text{lin}^3 * b * ac * x_1 * K_{I2} * \exp(-ac * x_1 * b) - 2 * x_3^2 * D * K_{I1} * b^3 * x_1^3 * ac^3 * K_{I2}^2 * \text{lin} * \exp(-ac * x_1 * b) - 4 * x_3^2 * D * K_{I1} * b^2 * x_1^2 * ac^2 * K_{I2} * \text{lin}^2 * \exp(-ac * x_1 * b) - \text{mumax} * \text{lin}^3 * b * ac * x_1^2 - 2 * x_3^2 * D * \text{lin}^3 * b * x_1 * ac * K_{I2} * \exp(-3 * ac * x_1 * b) + x_3 * \text{mumax} * \text{lin}^3 * \exp(-3 * ac * x_1 * b) * b^2 * x_1^2 * ac^2 * K_{I2} + x_3^2 * D * \text{lin}^4 + 2 * x_3^2 * \text{mumax} * \text{lin}^3 * b * ac * x_1 * K_{I2} * \exp(-3 * ac * x_1 * b) + \text{mumax} * \text{lin}^3 * b * ac * x_1^2 * \exp(-3 * ac * x_1 * b) - 2 * x_3^2 * \text{mumax} * \text{lin}^3 * \exp(-2 * ac * x_1 * b) * b^2 * x_1^2 * ac^2 * K_{I2} + 2 * x_3^2 * D * \text{lin}^3 * b * x_1 * ac * K_{I2} + x_3^2 * D * \text{lin}^2 * b^2 * x_1^2 * ac^2 * K_{I2}^2 - x_3 * \text{mumax} * \text{lin}^2 * b^2 * ac^2 * x_1^2 * K_{I2}^2 - 2 * x_3^2 * \text{mumax} * \text{lin}^3 * b * ac * x_1 * K_{I2} + x_3^2 * D * K_{I1}^2 * b^4 * x_1^4 * ac^4 * K_{I2}^2 + 2 * x_3^2 * D * K_{I1} * b^3 * x_1^3 * ac^3 * K_{I2}^2 * \text{lin} + 2 * x_3^2 * D * K_{I1} * b^2 * x_1^2 * ac^2 * K_{I2} * \text{lin}^2 + 2 * x_3^2 * D * K_{I1} * b^2 * x_1^2 * ac^2 * K_{I2} * \text{lin}^2 * \exp(-2 * ac * x_1 * b) - x_3 * \text{mumax} * \text{lin}^2 * b^2 * ac^2 * x_1^2 * K_{I2}^2 * \exp(-2 * ac * x_1 * b)) / ((K_{I1} * b^2 * x_1^2 * ac^2 * K_{I2} + \text{lin} * b * x_1 * ac * K_{I2} - \text{lin} * b * x_1 * ac * K_{I2} * \exp(-ac * x_1 * b) + \text{lin}^2 - 2 * \text{lin}^2 * \exp(-ac * x_1 * b) + \text{lin}^2 * \exp(-2 * ac * x_1 * b)) ^2$$

$$dx_4dt = - (2 * x_4^2 * D * K_{I1} * b^3 * x_1^3 * ac^3 * K_{I2}^2 * \text{lin} * \exp(-ac * x_1 * b) - 4 * x_4^2 * D * K_{I1} * b^2 * x_1^2 * ac^2 * K_{I2} * \text{lin}^2 * \exp(-ac * x_1 * b) - 2 * x_4^2 * D * \text{lin}^2 * b^2 * x_1^2 * ac^2 * K_{I2}^2 * \exp(-ac * x_1 * b) + \text{lin} * b^3 * ac^3 * x_1^4 * K_{I2}^2 * \exp(-ac * x_1 * b) * K_{I1} + x_4^2 * D * \text{lin}^4 * \exp(-4 * ac * x_1 * b) + 2 * \text{lin}^2 * b^2 * ac^2 * x_1^3 * K_{I2}^2 * \exp(-ac * x_1 * b) - 4 * x_4^2 * D * \text{lin}^4 * \exp(-3 * ac * x_1 * b) - \text{lin} * b^3 * ac^3 * x_1^4 * K_{I2}^2 * K_{I1} + 3 * \text{lin}^3 * b * ac * x_1^2 * K_{I2} * \exp(-ac * x_1 * b) - 6 * x_4^2 * D * \text{lin}^3 * b * x_1 * ac * K_{I2} * \exp(-ac * x_1 * b) - 4 * x_4^2 * D * \text{lin}^4 * \exp(-ac * x_1 * b) + 6 * x_4^2 * D * \text{lin}^4 * \exp(-2 * ac * x_1 * b) - x_4 * \text{mumax} * \text{lin} * \exp(-ac * x_1 * b) * b^4 * x_1^4 * ac^4 * K_{I2}^2 * K_{I1} + x_4 * \text{mumax} * \text{lin}^3 * \exp(-ac * x_1 * b) * b^2 * x_1^2 * ac^2 * K_{I2} + 2 * x_4^2 * \text{mumax} * \text{lin}^2 * b^2 * ac^2 * x_1^2 * K_{I2}^2 * \exp(-$$

$$\begin{aligned}
 & ac \cdot x_1 \cdot b) + 6 \cdot x_4 \cdot \text{mumax} \cdot \text{lin}^3 \cdot b \cdot ac \cdot x_1 \cdot K_{I2} \cdot \exp(- \\
 & ac \cdot x_1 \cdot b) + x_4 \cdot D \cdot \text{lin}^4 + 2 \cdot x_4 \cdot D \cdot \text{lin}^3 \cdot b \cdot x_1 \cdot ac \cdot K_{I2} + x_4 \cdot D \cdot \text{lin}^2 \cdot b^2 \cdot x_1^2 \cdot ac^2 \cdot K_{I2}^2 - \\
 & x_4 \cdot \text{mumax} \cdot \text{lin}^2 \cdot b^2 \cdot ac^2 \cdot x_1^2 \cdot K_{I2}^2 - \\
 & 2 \cdot x_4 \cdot \text{mumax} \cdot \text{lin}^3 \cdot b \cdot ac \cdot x_1 \cdot K_{I2} + x_4 \cdot D \cdot K_{I1}^2 \cdot b^4 \cdot x_1^4 \cdot ac^4 \cdot K_{I2}^2 + 2 \cdot x_4 \cdot D \cdot K_{I1} \cdot b^3 \cdot x_1^3 \cdot ac^3 \cdot \\
 & K_{I2}^2 \cdot \text{lin} + 2 \cdot x_4 \cdot D \cdot K_{I1} \cdot b^2 \cdot x_1^2 \cdot ac^2 \cdot K_{I2} \cdot \text{lin}^2 - \text{lin}^2 \cdot b^2 \cdot ac^2 \cdot x_1^3 \cdot K_{I2}^2 - \\
 & \text{lin}^3 \cdot b \cdot ac \cdot x_1^2 \cdot K_{I2} + 2 \cdot x_4 \cdot D \cdot K_{I1} \cdot b^2 \cdot x_1^2 \cdot ac^2 \cdot K_{I2} \cdot \text{lin}^2 \cdot \exp(- \\
 & 2 \cdot ac \cdot x_1 \cdot b) + 6 \cdot x_4 \cdot D \cdot \text{lin}^3 \cdot b \cdot x_1 \cdot ac \cdot K_{I2} \cdot \exp(-2 \cdot ac \cdot x_1 \cdot b) + x_4 \cdot D \cdot \text{lin}^2 \cdot b^2 \cdot x_1^2 \cdot ac^2 \cdot K_{I2}^2 \cdot \exp(- \\
 & 2 \cdot ac \cdot x_1 \cdot b) - 2 \cdot x_4 \cdot D \cdot \text{lin}^3 \cdot b \cdot x_1 \cdot ac \cdot K_{I2} \cdot \exp(-3 \cdot ac \cdot x_1 \cdot b) + \text{lin}^3 \cdot b \cdot ac \cdot x_1^2 \cdot K_{I2} \cdot \exp(-3 \cdot ac \cdot x_1 \cdot b) - \\
 & 3 \cdot \text{lin}^3 \cdot b \cdot ac \cdot x_1^2 \cdot K_{I2} \cdot \exp(-2 \cdot ac \cdot x_1 \cdot b) - \text{lin}^2 \cdot b^2 \cdot ac^2 \cdot x_1^3 \cdot K_{I2}^2 \cdot \exp(-2 \cdot ac \cdot x_1 \cdot b) - \\
 & 2 \cdot x_4 \cdot \text{mumax} \cdot \text{lin}^3 \cdot \exp(-2 \cdot ac \cdot x_1 \cdot b) \cdot b^2 \cdot x_1^2 \cdot ac^2 \cdot K_{I2} + x_4 \cdot \text{mumax} \cdot \text{lin}^3 \cdot \exp(- \\
 & 3 \cdot ac \cdot x_1 \cdot b) \cdot b^2 \cdot x_1^2 \cdot ac^2 \cdot K_{I2} - 6 \cdot x_4 \cdot \text{mumax} \cdot \text{lin}^3 \cdot b \cdot ac \cdot x_1 \cdot K_{I2} \cdot \exp(-2 \cdot ac \cdot x_1 \cdot b) - \\
 & x_4 \cdot \text{mumax} \cdot \text{lin}^2 \cdot b^2 \cdot ac^2 \cdot x_1^2 \cdot K_{I2}^2 \cdot \exp(-2 \cdot ac \cdot x_1 \cdot b) + 2 \cdot x_4 \cdot \text{mumax} \cdot \text{lin}^3 \cdot b \cdot ac \cdot x_1 \cdot K_{I2} \cdot \exp(- \\
 & 3 \cdot ac \cdot x_1 \cdot b) / (K_{I1} \cdot b^2 \cdot x_1^2 \cdot ac^2 \cdot K_{I2} + \text{lin} \cdot b \cdot x_1 \cdot ac \cdot K_{I2} - \text{lin} \cdot b \cdot x_1 \cdot ac \cdot K_{I2} \cdot \exp(-ac \cdot x_1 \cdot b) + \text{lin}^2 \cdot \\
 & 2 \cdot \text{lin}^2 \cdot \exp(-ac \cdot x_1 \cdot b) + \text{lin}^2 \cdot \exp(-2 \cdot ac \cdot x_1 \cdot b))^2
 \end{aligned}$$



### 9.3. Appendix 3. Analytical solution

```

In[1]= x1'[t] = μmax x2[t] / (KI + x2[t]) x1[t]
      x2'[t] = u[t]

Out[1]= 
$$\frac{\mu_{\max} x_1[t] x_2[t]}{KI + x_2[t]}$$


Out[2]= u[t]

In[3]= states = {x1[t], x2[t]}
      sens = {{x3[t], x4[t]}, {x5[t], x6[t]}}

Out[3]= {x1[t], x2[t]}

Out[4]= {{x3[t], x4[t]}, {x5[t], x6[t]}}

In[5]= S = Simplify[Outer[D, {x1'[t]}, states].sens + Outer[D, {x1'[t]}, {KI, μmax}]]

Out[5]= 
$$\left\{ \left\{ \frac{\mu_{\max} (x_2[t] (KI + x_2[t]) x_3[t] + x_1[t] (-x_2[t] + KI x_5[t]))}{(KI + x_2[t])^2}, \right. \right.$$


$$\left. \left. \frac{\mu_{\max} x_2[t] (KI + x_2[t]) x_4[t] + x_1[t] (KI x_2[t] + x_2[t]^2 + KI \mu_{\max} x_6[t])}{(KI + x_2[t])^2} \right\} \right\}$$


In[6]= sens // MatrixForm
      S // MatrixForm

Out[6]/MatrixForm=

$$\begin{pmatrix} x_3[t] & x_4[t] \\ x_5[t] & x_6[t] \end{pmatrix}$$


Out[7]/MatrixForm=

$$\begin{pmatrix} \frac{\mu_{\max} (x_2[t] (KI - x_2[t]) x_3[t] - x_1[t] (-x_2[t] - KI x_5[t]))}{(KI - x_2[t])^2} & \frac{\mu_{\max} x_2[t] (KI - x_2[t]) x_4[t] - x_1[t] (KI x_2[t] - x_2[t]^2 - KI \mu_{\max} x_6[t])}{(KI - x_2[t])^2} \end{pmatrix}$$


In[8]= x3'[t] = S[[1, 1]] /. x5[t] → 0

Out[8]= 
$$\frac{\mu_{\max} (-x_1[t] x_2[t] + x_2[t] (KI + x_2[t]) x_3[t])}{(KI + x_2[t])^2}$$


In[9]= H[t] = -(x3[t]^2) + λ1[t] x1'[t] + λ2[t] x2'[t] + λ3[t] x3'[t]

Out[9]= 
$$-x_3[t]^2 + \frac{\mu_{\max} x_1[t] x_2[t] \lambda_1[t]}{KI + x_2[t]} + u[t] \lambda_2[t] +$$


$$\frac{\mu_{\max} (-x_1[t] x_2[t] + x_2[t] (KI + x_2[t]) x_3[t]) \lambda_3[t]}{(KI + x_2[t])^2}$$


In[10]= λ1'[t] = -D[H[t], x1[t]]
        λ2'[t] = -D[H[t], x2[t]]
        λ3'[t] = -D[H[t], x3[t]]

Out[10]= 
$$-\frac{\mu_{\max} x_2[t] \lambda_1[t]}{KI + x_2[t]} + \frac{\mu_{\max} x_2[t] \lambda_3[t]}{(KI + x_2[t])^2}$$


Out[11]= 
$$\frac{\mu_{\max} x_1[t] x_2[t] \lambda_1[t]}{(KI + x_2[t])^2} - \frac{\mu_{\max} x_1[t] \lambda_1[t]}{KI + x_2[t]} -$$


$$\frac{\mu_{\max} (-x_1[t] + x_2[t] x_3[t] + (KI + x_2[t]) x_3[t]) \lambda_3[t]}{(KI + x_2[t])^2} +$$


$$\frac{2 \mu_{\max} (-x_1[t] x_2[t] + x_2[t] (KI + x_2[t]) x_3[t]) \lambda_3[t]}{(KI + x_2[t])^3}$$


Out[12]= 
$$2 x_3[t] - \frac{\mu_{\max} x_2[t] \lambda_3[t]}{KI + x_2[t]}$$


```

In[13]= eqn = Simplify[Table[D[D[H[t], u[t]], {t, i}], {i, 0, 2}]]

$$\text{Out[13]} = \left\{ \lambda_2[t], -\frac{1}{(KI + x_2[t])^3}, \mu_{\max} (KI (KI + x_2[t]) x_3[t] \lambda_3[t] + x_1[t] (KI (KI + x_2[t]) \lambda_1[t] + (-KI + x_2[t]) \lambda_3[t])), \frac{1}{(KI + x_2[t])^4} - 2 \mu_{\max} (-KI (KI + x_2[t]) x_3[t] ((KI + x_2[t]) x_3[t] - u[t] \lambda_3[t]) + x_1[t] ((KI^2 - x_2[t]^2) x_3[t] + u[t] (KI (KI + x_2[t]) \lambda_1[t] + (-2 KI + x_2[t]) \lambda_3[t]))) \right\}$$

In[14]= costates = {\lambda1[t], \lambda2[t], \lambda3[t]}

Out[14]= {\lambda1[t], \lambda2[t], \lambda3[t]}

In[15]= solcostates = Solve[eqn == 0, costates]

$$\text{Out[15]} = \left\{ \left\{ \lambda_2[t] \rightarrow 0, \lambda_1[t] \rightarrow \frac{x_3[t] (-KI x_1[t] + x_1[t] x_2[t] + KI^2 x_3[t] + KI x_2[t] x_3[t])^2}{KI^2 u[t] x_1[t]^2}, \lambda_3[t] \rightarrow -\frac{1}{KI u[t] x_1[t]} \right. \right. \\ \left. \left. (-KI^2 x_1[t] x_3[t] + x_1[t] x_2[t]^2 x_3[t] + KI^3 x_3[t]^2 + 2 KI^2 x_2[t] x_3[t]^2 + KI x_2[t]^2 x_3[t]^2) \right\} \right\}$$

In[16]= A = Table[Coefficient[eqn[[i]], {\lambda1[t], \lambda2[t], \lambda3[t]}], {i, 3}]

$$\text{Out[16]} = \left\{ \{0, 1, 0\}, \left\{ -\frac{\mu_{\max} (KI^2 x_1[t] + KI x_1[t] x_2[t])}{(KI + x_2[t])^3}, 0, -\frac{\mu_{\max} (-KI x_1[t] + x_1[t] x_2[t] + KI^2 x_3[t] + KI x_2[t] x_3[t])}{(KI + x_2[t])^3} \right\}, \left\{ \frac{2 \mu_{\max} (KI^2 u[t] x_1[t] + KI u[t] x_1[t] x_2[t])}{(KI + x_2[t])^4}, 0, \frac{1}{(KI + x_2[t])^4} \right. \right. \\ \left. \left. 2 \mu_{\max} (-2 KI u[t] x_1[t] + u[t] x_1[t] x_2[t] + KI^2 u[t] x_3[t] + KI u[t] x_2[t] x_3[t]) \right\} \right\}$$

In[17]= A // MatrixForm

$$\text{Out[17]} // \text{MatrixForm} = \begin{pmatrix} 0 & 1 & 0 \\ -\frac{\mu_{\max} \{KI^2 x_1[t] - KI x_1[t] x_2[t]\}}{(KI + x_2[t])^3} & 0 & -\frac{\mu_{\max} \{-KI x_1[t] - x_1[t] x_2[t] - KI^2 x_3[t] - KI x_2[t] x_3[t]\}}{(KI + x_2[t])^3} \\ \frac{2 \mu_{\max} \{KI^2 u[t] x_1[t] - KI u[t] x_1[t] x_2[t]\}}{(KI + x_2[t])^4} & 0 & \frac{2 \mu_{\max} \{-2 KI u[t] x_1[t] - u[t] x_1[t] x_2[t] - KI^2 u[t] x_3[t] - KI u[t] x_2[t] x_3[t]\}}{(KI + x_2[t])^4} \end{pmatrix}$$

In[18]= B = Simplify[A]

$$\text{Out[18]} = \left\{ \{0, 1, 0\}, \left\{ -\frac{KI \mu_{\max} x_1[t]}{(KI + x_2[t])^2}, 0, -\frac{\mu_{\max} (x_1[t] (-KI + x_2[t]) + KI (KI + x_2[t]) x_3[t])}{(KI + x_2[t])^3} \right\}, \left\{ \frac{2 KI \mu_{\max} u[t] x_1[t]}{(KI + x_2[t])^3}, 0, \frac{2 \mu_{\max} u[t] (x_1[t] (-2 KI + x_2[t]) + KI (KI + x_2[t]) x_3[t])}{(KI + x_2[t])^4} \right\} \right\}$$

In[19]= Simplify[Det[B]]

$$\text{Out[19]} = -\frac{2 KI^2 \mu_{\max}^2 u[t] x_1[t]^2}{(KI + x_2[t])^6}$$

In[20]= uopt = Simplify[Solve[Det[B] == 0, u[t]]]

Out[20]= {{u[t] -> 0}}

In[21]= `SingArc = Simplify[H[t] /. solcostates]`

$$\text{Out[21]= } \left\{ \left\{ x_3[t] \left( \mu_{\max} x_1[t] x_2[t]^2 (-KI + x_2[t]) - KI (KI + x_2[t]) (KI u[t] - \mu_{\max} x_2[t]^2) x_3[t] \right) \right\} / \left( KI^2 u[t] (KI + x_2[t]) \right) \right\}$$

In[22]= `FullSimplify[Solve[(H[t] /. solcostates) == 0, x1[t]]]`

$$\text{Out[22]= } \left\{ \left\{ x_1[t] \rightarrow - \frac{KI (KI + x_2[t]) (KI u[t] - \mu_{\max} x_2[t]^2) x_3[t]}{\mu_{\max} (KI - x_2[t]) x_2[t]^2} \right\} \right\}$$

In[23]= `uoptdirect = DSolve[{u'[t] == x2'[t] /. uopt /. x2[t] -> u[t], u[0] == 102.5}, u[t], t]`

Out[23]= `{u[t] -> 102.5}`

In[24]= `eqnDsol = {y1'[t] == x1'[t], y2'[t] == x2'[t], y3'[t] == x3'[t][[1]]} /. uopt /. Thread[{x1[t], x2[t], x3[t]} -> {y1[t], y2[t], y3[t]}`

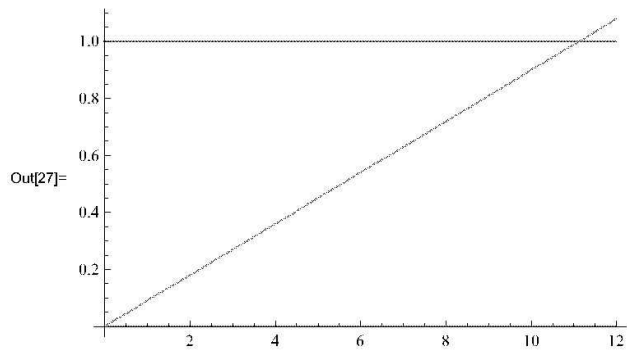
$$\text{Out[24]= } \left\{ \left\{ y_1'[t] = \frac{\mu_{\max} y_1[t] y_2[t]}{KI + y_2[t]}, y_2'[t] = 0, y_3'[t] = \mu_{\max} \right\} \right\}$$

In[25]= `Clear[t]`

In[26]= `sol = DSolve[{eqnDsol[[1]], y1[0] == 1, y2[0] == 0, y3[0] == 0}, {y1, y2, y3}, t]`

Out[26]= `{y2 -> Function[{t}, 0], y1 -> Function[{t}, 1], y3 -> Function[{t}, t \mu_{\max}]}`

In[27]= `Plot[Evaluate[{y1[t], y2[t], y3[t]} /. sol /. KI -> 69.86 /. \mu_{\max} -> 0.09], {t, 0, 12}, PlotRange -> {All, All}]`



### 9.4. Appendix 4. Tables of experimental design

**Table 3. Comparison of weighting factors**

S $K_I$ : S $\mu_{max}$ = q1 : q2							
weighting factor		0:1		1:0		1:1	
noise		0%	1%	0%	1%	0%	1%
given parameter in generated data	$\mu_{max}$	0.090	0.090	0.090	0.090	0.090	0.090
	$K_I$	69.86	69.86	69.86	69.86	69.86	69.86
initial guess parameter	$\mu_{max}$	0.01	0.01	0.01	0.01	0.01	0.01
	$K_I$	10	10	10	10	10	10
confidential interval	$\mu_{max}$ high	0.0905	137.9518	0.09	0.0982	0.0905	65.9833
	$\mu_{max}$ low	0.0903	-137.7696	0.09	0.0412	0.0903	-65.8038
estimated parameter	$\mu_{max}$	<b>0.0904</b>	<b>0.0911</b>	<b>0.09</b>	<b>0.0697</b>	<b>0.0904</b>	<b>0.0898</b>
confidential interval	$K_I$ high	78.9146	2.4061E+06	69.8596	85.8919	78.9146	1.1490E+06
	$K_I$ low	75.0465	-2.4059E+06	69.8594	-25.3547	75.0465	-1.1489E+06
estimated parameter	$K_I$	<b>76.9806</b>	<b>89.8435</b>	<b>69.8595</b>	<b>30.2686</b>	<b>76.9806</b>	<b>65.1978</b>
sensitivity value of $\mu_{max}$		<b>32.1793</b>		<b>14.0105</b>		<b>32.1793</b>	
sensitivity value of $K_I$		<b>-0.0018</b>		<b>-0.0071</b>		<b>-0.0018</b>	
cost function J		<b>2.6544E+03</b>		<b>1.4996E-04</b>		<b>2.6544E+03</b>	

**Table 4. Light intensity trajectories by using Monod model with 12 hours cultivation**

light intensity		constant 1 (- noise)	constant 1 (+ noise)	constant 2 (- noise)	constant 2 (+ noise)	stepwise (- noise)	stepwise (+ noise)	linear increasing (- noise)	linear increasing (+ noise)	optimised (- noise)	optimised (+ noise)
light intensity trajectory		constant 1		constant 2		stepwise		linear increasing		optimised	
noise application		0%	1%	0%	1%	0%	1%	0%	1%	0%	1%
light intensity ( $\mu\text{mol}/\text{m}^2\text{s}$ )	$I$	102.5	102.5	118	118	102.5 and 118	102.5 and 118	from 102.5 to 118	from 102.5 to 118	from 102.5 to 118	from 102.5 to 118
time span (h)	$t$	12	12	12	12	12	12	12	12	12	12
given parameter in generated data	$\mu_{max}$	0.090	0.090	0.090	0.090	0.090	0.090	0.090	0.090	0.090	0.090
	$K_I$	69.86	69.86	69.86	69.86	69.86	69.86	69.86	69.86	69.86	69.86
initial guess parameter	$\mu_{max}$	0.01	0.01	0.01	0.01	0.01	0.01	0.01	0.01	0.01	0.01
	$K_I$	10	10	10	10	10	10	10	10	10	10
confidential interval	$\mu_{max}$ high	0.1261	407.7452	0.1244	677.3865	0.0900	0.1535	0.0900	0.293	0.0900	0.1176
	$\mu_{max}$ low	0.0064	-407.6126	0.0132	-677.2496	0.0900	0.0638	0.0900	-0.0031	0.0900	0.0383
estimated parameter	$\mu_{max}$	<b>0.0662</b>	<b>0.0663</b>	<b>0.0688</b>	<b>0.0684</b>	<b>0.0900</b>	<b>0.1087</b>	<b>0.0900</b>	<b>0.145</b>	<b>0.0900</b>	<b>0.078</b>
confidential interval	$K_I$ high	138.9074	7.81E+05	141.6475	1.41E+06	69.8465	195.5567	69.8299	475.1789	69.8596	123.4584
	$K_I$ low	-90.3376	-7.81E+05	-90.458	-1.41E+06	69.8275	18.2546	69.7954	-114.8421	69.8594	-31.1548
estimated parameter	$K_I$	24.2849	<b>24.4474</b>	<b>25.5948</b>	<b>24.3112</b>	<b>69.8370</b>	<b>106.9057</b>	<b>69.8127</b>	<b>180.1684</b>	<b>69.8595</b>	<b>46.1518</b>
fitting tolerance		1.E-10	1.E-10	1.E-10	1.E-10	1.E-10	1.E-10	1.E-10	1.E-10	1.E-10	1.E-10
sensitivity value of $K_I$		<b>-0.0071</b>	<b>-0.0071</b>	<b>-0.0071</b>	<b>-0.0071</b>	<b>-0.0071</b>	<b>-0.0071</b>	<b>-0.0071</b>	<b>-0.0071</b>	<b>-0.0071</b>	<b>-0.0071</b>
sensitivity value of $\mu_{max}$		<b>13.5643</b>	<b>13.5643</b>	<b>14.854</b>	<b>14.854</b>	<b>14.1946</b>	<b>14.1946</b>	<b>14.2184</b>	<b>14.2184</b>	<b>14.0105</b>	<b>14.0105</b>
cost function J		<b>1.4979E-04</b>	<b>1.4979E-04</b>	<b>0.00014898</b>	<b>0.00014898</b>	<b>1.4981E-04</b>	<b>1.4981E-04</b>	<b>1.4990E-04</b>	<b>1.4990E-04</b>	<b>1.4996E-04</b>	<b>1.4996E-04</b>

**Table 5. Light intensity trajectories by using Monod model for 25 hours cultivation (noise free)**

light intensity		constant 1		constant 2		stepwise		linear increasing		optimised	
light intensity ( $\mu\text{mol}/\text{m}^2\text{s}$ )	I	155.3418	155.3418	194	194	155.3418 and 194	155.3418 and 194	From 155.3418 to 194	From 155.3418 to 194	From 155.3418 to 194	From 155.3418 to 194
time span (h)	t	25	25	25	25	25	25	25	25	25	25
given parameter in generated data	$\mu_{max}$	0.090	0.090	0.090	0.090	0.090	0.090	0.090	0.090	0.090	0.090
	$K_I$	69.86	69.86	69.86	69.86	69.86	69.86	69.86	69.86	69.86	69.86
initial guess parameter	$\mu_{max}$	0.01	0.01	0.01	0.01	0.01	0.01	0.01	0.01	0.01	0.01
	$K_I$	10	10	10	10	10	10	10	10	10	10
confidential interval	$\mu_{max}$ high	0.0956	0.0662	0.0967	0.0697	0.09	0.09	0.09	0.09	0.09	0.09
	$\mu_{max}$ low	0.0368	0.0662	0.0427	0.0697	0.09	0.09	0.09	0.09	0.09	0.09
estimated parameter	$\mu_{max}$	<b>0.0662</b>	<b>0.0662</b>	<b>0.0697</b>	<b>0.0697</b>	<b>0.09</b>	<b>0.09</b>	<b>0.09</b>	<b>0.09</b>	<b>0.09</b>	<b>0.09</b>
confidential interval	$K_I$ high	83.9749	10.3358	89.5741	10.3769	69.8591	69.86	69.8599	69.8492	69.852	69.86
	$K_I$ low	-63.3096	10.3281	-68.826	10.3683	69.8481	69.86	69.8407	69.8461	69.848	69.86
estimated parameter	$K_I$	<b>10.3326</b>	<b>10.3319</b>	<b>10.3741</b>	<b>10.3726</b>	<b>69.8536</b>	<b>69.86</b>	<b>69.8503</b>	<b>69.8476</b>	<b>69.85</b>	<b>69.86</b>
fitting tolerance		1.E-10	1.E-10	1.E-10	1.E-10	1.E-10	1.E-10	1.E-10	1.E-10	1.E-10	1.E-10
amount of data		101	251	101	251	101	251	101	251	101	251
sensitivity value of $K_I$		<b>-0.0325</b>	<b>-0.0325</b>	<b>-0.0328</b>	<b>-0.0328</b>	<b>-0.0327</b>	<b>-0.0327</b>	<b>-0.0328</b>	<b>-0.0328</b>	<b>-0.0327</b>	<b>-0.0327</b>
sensitivity value of $\mu_{max}$		<b>81.4128</b>	<b>81.4128</b>	<b>96.1204</b>	<b>96.1204</b>	<b>88.4787</b>	<b>88.4787</b>	<b>88.8949</b>	<b>88.8949</b>	<b>85.407</b>	<b>85.407</b>
cost function J		<b>4.700E-03</b>	<b>4.700E-03</b>	<b>4.600E-03</b>	<b>4.600E-03</b>	<b>4.7171E-03</b>	<b>4.7171E-03</b>	<b>4.723E-03</b>	<b>4.723E-03</b>	<b>4.7323E-03</b>	<b>4.7323E-03</b>

**Table 6. Light intensity trajectories by using Monod model and Lambert-Beer law**

light intensity		constant 1 (- noise)	constant 1 (+ noise)	constant 2 (- noise)	constant 2 (+ noise)	stepwise (- noise)	stepwise (+ noise)	linear increasing (- noise)	linear increasing (+ noise)	optimised (- noise)	optimised (+ noise)
light intensity trajectory		constant 1		constant 2		stepped		increased		optimised	
noise application		0%	1%	0%	1%	0%	1%	0%	1%	0%	1%
light intensity ( $\mu\text{mol}/\text{m}^2\text{s}$ )	I	634	634	1484	1484	634 and 1484	634 and 1484	from 634 to 1484	from 634 to 1484	from 634 to 1484	from 634 to 1484
time span (h)	t	12	12	12	12	12	12	12	12	12	12
given parameter in generated data	$\mu_{max}$	0.090	0.090	0.090	0.090	0.09	0.09	0.09	0.09	0.09	0.09
	$K_I$	69.86	69.86	69.86	69.86	69.86	69.86	69.86	69.86	69.86	69.86
initial guess parameter	$\mu_{max}$	0.01	0.01	0.01	0.01	0.01	0.01	0.01	0.01	0.01	0.01
	$K_I$	10	10	10	10	10	10	10	10	10	10
confidential interval	$\mu_{max}$ high	0.09	0.0991	0.09	0.089	0.09	0.0939	0.09	0.1095	0.09	0.0976
	$\mu_{max}$ low	0.09	0.0687	0.09	0.078	0.09	0.0765	0.09	0.0446	0.09	0.0501
estimated parameter	$\mu_{max}$	<b>0.09</b>	<b>0.0839</b>	<b>0.09</b>	<b>0.0835</b>	<b>0.09</b>	<b>0.0852</b>	<b>0.09</b>	<b>0.0771</b>	<b>0.09</b>	<b>0.0738</b>
confidential interval	$K_I$ high	69.8684	85.6335	69.8724	66.5656	69.8582	78.4786	69.852	110.8656	69.8597	85.0723
	$K_I$ low	69.8646	33.7761	69.8667	36.1124	69.854	43.1935	69.8192	-26.356	69.8595	-9.8863
estimated parameter	$K_I$	<b>69.8665</b>	<b>59.7048</b>	<b>69.8695</b>	<b>51.339</b>	<b>69.8561</b>	<b>60.836</b>	<b>69.8356</b>	<b>42.2548</b>	<b>69.8596</b>	<b>32.293</b>
fitting tolerance		1.E-05	1.E-05	1.E-05	1.E-05	1.E-05	1.E-05	1.E-05	1.E-05	1.E-05	1.E-05
sensitivity value of $K_I$		<b>-0.0059</b>	<b>-0.0059</b>	<b>-0.0061</b>	<b>-0.0061</b>	<b>-0.0062</b>	<b>-0.0062</b>	<b>-0.0063</b>	<b>-0.0063</b>	<b>-0.0063</b>	<b>-0.0063</b>
sensitivity value of $\mu_{max}$		<b>9.7863</b>	<b>9.7863</b>	<b>15.9873</b>	<b>15.9873</b>	<b>13.072</b>	<b>13.072</b>	<b>13.4428</b>	<b>13.4428</b>	<b>12.7529</b>	<b>12.7529</b>
cost function J		<b>1.1670E-04</b>	<b>1.1670E-04</b>	<b>1.0771E-04</b>	<b>1.0771E-04</b>	<b>1.1973E-04</b>	<b>1.1973E-04</b>	<b>1.2232E-04</b>	<b>1.2232E-04</b>	<b>1.2287E-04</b>	<b>1.2287E-04</b>

**Table 7. Light intensity trajectories by using Haldane model and Lambert-Beer law**

		S K1 : S K2 : S Mumax = q <sub>1</sub> : q <sub>2</sub> : q <sub>3</sub>					
weighting factors		1E8:0:0		0:1E8:0		0:0:1E8	
noise		without	with	without	with	without	with
time span (h)	t	12	12	12	12	12	12
noise	%	0%	1%	0%	1%	0%	1%
given parameter in generated data	$\mu_{max}$	0.09	0.09	0.09	0.09	0.09	0.09
	$K_1$	69.86	69.86	69.86	0	0	0
	$K_2$	10	10	10	0	0	0
initial guess parameter	$\mu_{max}$	0.08	0.08	0.08	0.08	0.08	0.08
	$K_1$	69	69	69	69	69	69
	$K_2$	9	9	9	9	9	9
confidential interval	$\mu_{max}$ high	0.1126	39.5042	0.1757	184.3894	0.0923	7.3244
	$\mu_{max}$ low	0.0658	-39.3214	0.0028	-184.1966	0.0859	-7.1364
estimated parameter	$\mu_{max}$	0.0892	0.0914	0.0892	0.0964	0.0891	0.094
confidential interval	$K_1$ high	89.2152	3.30E+04	160.2763	1.80E+05	72.0081	6.46E+03
	$K_1$ low	49.159	-3.28E+04	-22.0325	-1.79E+05	66.0435	-6.32E+03
estimated parameter	$K_1$	69.1871	68.9912	69.1219	69.0013	69.0258	69.0001
confidential interval	$K_2$ high	13.6967	5.04E+03	20.8777	1.88E+04	10.5481	8.12E+02
	$K_2$ low	6.5577	-5.02E+03	-0.6794	-1.88E+04	9.6919	-7.94E+02
estimated parameter	$K_2$	10.1272	8.9385	10.0991	9.0153	10.12	9.0003
fitting tolerance		1.E-05	1.E-05	1.E-05	1.E-05	1.E-05	1.E-05
sensitivity value of K1		<b>-0.0016</b>	<b>-0.0016</b>	<b>-0.00047575</b>	<b>-0.00047575</b>	<b>-0.0011</b>	<b>-0.0011</b>
sensitivity value of K2		<b>0.0034</b>	<b>0.0034</b>	<b>0.0118</b>	<b>0.0118</b>	<b>0.0092</b>	<b>0.0092</b>
sensitivity value of $\mu_{max}$		<b>1.8637</b>	<b>1.8637</b>	<b>1.9477</b>	<b>1.9477</b>	<b>2.2746</b>	<b>2.2746</b>
cost function J		<b>9.4577E+02</b>	<b>9.4577E+02</b>	<b>5.1264E+04</b>	<b>5.1264E+04</b>	<b>1.8985E+09</b>	<b>1.8985E+09</b>

## 9.5. Appendix 5. Program scripts

The scripts are compiled in a CD which is included in this thesis. It has some files as follows:

- General files
  - clip : a function for clipping input arrays
  - derivation : derive parametric sensitivity equations
  - fop0 : a function optimisation by using Bryson method that perform some iterations
  - fop0\_b : subroutine of fop0 that perform backward integration
  - fop0\_f : subroutine of fop0 that perform forward integration
  - linvf\_u\_vec : differentiate a vector function of x, u, and theta with respect to u
  - linvf\_x\_vec : differentiate a vector function of x, u, and theta with respect to x
  - mysurface : provide mesh and contour plot with 10% interval
- Monod model files
  - fitfunA : calculate error between model and measurement values based on Bryson approach with Monod model
  - fitfunPW : calculate error between model and measurement values based on piecewise linear approach with Monod and extended Monod model
  - fittingA : estimate parameter  $\mu_{\max}$  and  $K_I$  based on Bryson approach with Monod model
  - fittingPW : estimate parameter  $\mu_{\max}$  and  $K_I$  based on piecewise linear approach with Monod and extended Monod model
  - functionA : a function which has calculation switch of cost function to determine forward and backward integration by using Monod model
  - functionPW\_A : a function contains cost function calculation for piecewise linear approach by using Monod model
  - functionPW F\_A: a function which calculate state variables and input values from optimised input values for piecewise linear approach by using Monod model
  - modelA : Monod model for Bryson approach
  - modelPW\_A : Monod model for piecewise linear approach
  - sensitivityA : perform input optimisation with Bryson approach by using Monod model
  - sensPW\_A : perform input optimisation with piecewise linear approach by using Monod model
  - testmodelA : perform simulation with constant, stepwise and linear increasing input trajectories by using extended Monod model
- Extended Monod model files
  - fitfunB : estimate parameter  $\mu_{\max}$  and  $K_I$  based on Bryson approach with extended Monod model
  - fitfunPW : calculate error between model and measurement values based on piecewise linear approach with Monod and extended Monod model
  - fittingB : estimate parameter  $\mu_{\max}$  and  $K_I$  based on Bryson approach with extended Monod model
  - fittingPW : estimate parameter  $\mu_{\max}$  and  $K_I$  based on piecewise linear approach with Monod and extended Monod model
  - functionB : a function which has calculation switch of cost function to determine forward and backward integration by using extended Monod model
  - functionPW\_B : a function contains cost function calculation for piecewise linear approach by using extended Monod model
  - functionPW F\_B: a function which calculate state variables and input values from optimised input values for piecewise linear approach by using extended Monod model
  - modelB : extended Monod model for Bryson approach

- modelPW\_B : extended Monod model for piecewise linear approach
- sensitivityB : perform input optimisation with Bryson approach by using extended Monod model
- sensPW\_B : perform input optimisation with piecewise linear approach by using extended Monod model
- testmodelB : perform simulation with constant, stepwise and linear increasing input trajectories by using extended Monod model
  
- Extended Haldane model files
  - fitfunC : estimate parameter  $\mu_{\max}$ ,  $K_1$  and  $K_2$  based on Bryson approach with extended Haldane model
  - fitfunPW\_C : calculate error between model and measurement values based on piecewise linear approach extended Haldane model
  - fitfunPW\_C1P : calculate error between model and measurement values based on piecewise linear approach with extended Haldane model
  - fitfunPW\_C2P : calculate error between model and measurement values based on piecewise linear approach with extended Haldane model
  - fittingC : estimate parameter  $\mu_{\max}$ ,  $K_1$  and  $K_2$  based on Bryson approach with extended Haldane model
  - fittingPW\_C : estimate parameter  $\mu_{\max}$ ,  $K_1$  and  $K_2$  based on piecewise linear approach with extended Haldane model
  - fittingPW\_C1P : estimate parameter one of  $\mu_{\max}$  or  $K_1$  or  $K_2$  based on piecewise linear approach with extended Haldane model
  - fittingPW\_C2P : estimate parameter two combination of parameters based on piecewise linear approach with extended Haldane model
  - fittingPW\_C\_ID : estimate parameter  $\mu_{\max}$ ,  $K_1$  and  $K_2$  based on piecewise linear approach with extended Haldane model
  - functionC : a function which has calculation switch of cost function to determine forward and backward integration by using extended Haldane model
  - functionPW\_C : a function contains cost function calculation for piecewise linear approach by using extended Haldane model
  - functionPW\_C\_ID : a function contains cost function calculation for piecewise linear approach by using extended Haldane model for 2 inputs optimisation
  - functionPW F\_C : a function which calculate state variables and input values from optimised input values for piecewise linear approach by using extended Haldane model
  - functionPW F\_C\_ID : a function which calculate state variables and input values from optimised input values for piecewise linear approach by using extended Haldane model for 2 inputs optimisation
  - modelC : extended Haldane model for Bryson approach
  - modelPW\_C : extended Haldane model for piecewise linear approach
  - modelPW\_C1P : extended Haldane model for piecewise linear approach for estimating 1 parameter only
  - modelPW\_C2P : extended Haldane model for piecewise linear approach for estimating 2 parameters
  - modelPW\_C\_ID : extended Haldane model for piecewise linear approach for 2 inputs optimisation
  - sensitivityC : perform input optimisation with Bryson approach by using extended Haldane model
  - sensPW\_C : perform light intensity input optimisation with piecewise linear approach by using extended Haldane model
  - sensPW\_C\_ID : perform light intensity and dilution inputs optimisation with piecewise linear approach by using extended Haldane model
  - testmodelC : perform simulation with constant, stepwise and linear increasing input trajectories by using extended Haldane model